AD-A010 046

USE OF HIGH ENERGY, SHORT PULSE EXPLOSIVE GENERATORS TO DRIVE ELECTROMAGNETIC IMPLOSIONS

Peter J. Turchi, et al

Air Force Weapons Laboratory
Kirtland Air Force Base, New Mexico

April 1975

AFWL-TR-
74-222

USE OF HIGH ENERGY, SHORT PULSE EXPLOSIVE GENERATORS TO DRIVE ELECTROMAGNETIC IMPLOSIONS

Robert S. Caird
Los Alamos Scientific Laboratory
Los Alamos, New Mexico

Peter J. Turchi

April 1975

Final Report for Period July 1971 - September 1973

Approved for public release; distribution unlimited.

AIR FORCE WEAPONS LABORATORY
Air Force Systems Command
Kirtland Air Force Base, NM 87117

UNCLASSIFIED
SECURITY CLASSIFICATION OF THIS PAGE (When Data Entered)

REPORT DOCUMENTATION PAGE

READ INSTRUCTIONS BEFORE COMPLETING FORM

1. REPORT NUMBER: AFWL-TR-74-222
2. GOVT ACCESSION NO.:
3. RECIPIENT'S CATALOG NUMBER: AD-A010046

4. TITLE (and Subtitle): USE OF HIGH ENERGY, SHORT PULSE EXPLOSIVE GENERATORS TO DRIVE ELECTROMAGNETIC IMPLOSIONS

5. TYPE OF REPORT & PERIOD COVERED: Final Report July 1971 - September 1973

6. PERFORMING ORG. REPORT NUMBER:

7. AUTHOR(s): Peter J. Turchi (AFWL); Robert S. Caird (LASL)

8. CONTRACT OR GRANT NUMBER(s):

9. PERFORMING ORGANIZATION NAME AND ADDRESS: Air Force Weapons Laboratory, Kirtland Air Force Base, NM 87117

10. PROGRAM ELEMENT, PROJECT, TASK AREA & WORK UNIT NUMBERS: ILIR7203

11. CONTROLLING OFFICE NAME AND ADDRESS: Air Force Weapons Laboratory, Kirtland Air Force Base, NM 87117

12. REPORT DATE: April 1975

13. NUMBER OF PAGES: ~~50~~ 61

14. MONITORING AGENCY NAME & ADDRESS (if different from Controlling Office): Air Force Weapons Laboratory, Kirtland Air Force Base, NM 87117

15. SECURITY CLASS. (of this report): UNCLASSIFIED

15a. DECLASSIFICATION/DOWNGRADING SCHEDULE:

16. DISTRIBUTION STATEMENT (of this Report): Approved for public release; distribution unlimited.

17. DISTRIBUTION STATEMENT (of the abstract entered in Block 20, if different from Report): Same as block 16.

18. SUPPLEMENTARY NOTES:

19. KEY WORDS (Continue on reverse side if necessary and identify by block number):
Explosive Generator
Electromagnetic Implosion
Plasmas
Radiation
Magnetic Fields

20. ABSTRACT (Continue on reverse side if necessary and identify by block number):

The feasibility of using high energy (~ 5 MJ), short pulse time (~ 2 μsec) explosive generators to drive electromagnetic implosions is investigated theoretically. Detailed calculations show that the generated energy can be transferred to imploding plasma discharges with efficiencies exceeding 50 percent. The creation of multimegajoule plasmas is possible using moderate amounts of high explosive (~ 25 kg). By employing more generators, plasma implosion speeds in excess of 100 cm/μsec and kinetic energies exceeding 10 MJ are computed. (OVER)

DD FORM 1 JAN 73 1473 EDITION OF 1 NOV 65 IS OBSOLETE.

UNCLASSIFIED

SECURITY CLASSIFICATION OF THIS PAGE (When Data Entered)

ABSTRACT (Cont'd)

Such plasmas can be used to compress other plasmas and/or magnetic fields or to produce high power prompt radiation at levels in excess of 10^{14} W. Practical factors limiting generator performance are considered in detail. Specific areas of concern include resistive heating, internal arcing, and conductor dynamics. Two types of generator designs are investigated, both based on plane detonation systems. One design is a parallel plate generator and the other a new coaxial configuration. Relative advantages and disadvantages are discussed and some initial experimental work related to the new design is presented.

This final report was prepared by the Air Force Weapons Laboratory, Kirtland Air Force Base, New Mexico and Los Alamos Scientific Laboratory, Los Alamos, New Mexico, Job Order ILIR7203. Dr. W. L. Baker (CYS) was the Laboratory Project Officer-in-Charge.

When US Government drawings, specifications, or other data are used for any purpose other than a definitely related Government procurement operation, the Government thereby incurs no responsibility nor any obligation whatsoever, and the fact that the Government may have formulated, furnished, or in any way supplied the said drawings, specifications, or other data, is not to be regarded by implication or otherwise, as in any manner licensing the holder or any other person or corporation, or conveying any rights or permission to manufacture, use, or sell any patented invention that may in any way be related thereto.

This technical report has been reviewed and is approved for publication.

William L. Baker

WILLIAM L. BAKER
Project Officer

THOMAS C. MAY
Major, USAF
Chief, X-Ray Simulation Branch

DAVID M ERICSON, JR.
Lt Colonel, USAF
Chief, Technology Division

DO NOT RETURN THIS COPY. RETAIN OR DESTROY.

CONTENTS

SECTION I

INTRODUCTION

Multimegajoule, high temperature plasmas are of interest for a variety of applications ranging from controlled thermonuclear fusion to nuclear weapons radiation simulation. This report considers the feasibility of using high energy, short pulse explosive generators as power sources for the creation of such plasmas by the implosion of thin, metallic foil cylinders through $\vec{j} \times \vec{B}$ forces. The goal of this study has been to ascertain the possibility of developing explosive generators capable of providing the necessary energies ($\sim$ 5 MJ) and currents ($\sim$ 50 MA) in the short pulse times ($\sim$ 2 μsec) required by this method of generating multimegajoule, high temperature plasmas. The approach followed has been two-fold: numerical computation of the performance of various explosive generator and electromagnetic implosion configurations; and intensive qualitative discussion of experimental phenomena present in these systems but not amenable to detail analytical or numerical treatment. Of particular concern have been practical considerations limiting or otherwise affecting generator performances, such as internal arcing, conductor jetting, and resistive heating, as well as design problems such as explosive utilization and system cost. While the primary motivation for this study has been the need for high power, prompt radiation sources for nuclear weapons effects testing, the high energy, high speed, imploding plasmas described here should also find applications elsewhere.

SECTION II

ELECTROMAGNETIC IMPLOSION

Of primary importance in the development of an explosive generator power source is the nature of the electrical load to be driven. The load of interest in the present work is a dynamic plasma discharge, similar to a fast Z-pinch, known as an electromagnetic (EM) implosion. Calculations (ref. 1) indicate that such discharges can be coupled very efficiently to fast, high energy, high current electrical power systems to provide high power, high energy radiation sources.

The approach is to obtain a very energetic high Z plasma by passing a current of more than 20 MA through a large radius, thin foil cylinder. The thin foil ($\sim$ 1 μm thick) becomes a plasma a few millimeters thick very early in the current pulse and then implodes at high speed under the influence of the $\vec{j} \times \vec{B}$ force. Electrical energy delivered to the plasma appears primarily as radially directed kinetic energy which is not radiated appreciably. Thus, high kinetic energies per particle can be obtained. When the plasma collapses on itself at the implosion center, the accumulated kinetic energy is converted with high efficiency to thermal energy which, because of the high density (> 1 percent solid density) and temperature, will be radiated in a very short burst. A schematic description of the process is shown in figure 1. The rate of energy delivery to plasma thermal energy is essentially limited only by hydrodynamic times. The radiation rate can, therefore, be increased (over that which can be obtained by direct energy delivery to plasma internal energy from the power supply) by the ratio of current pulse time to hydrodynamic time, a factor of about 100. This approach assumes that energy can be transferred efficiently from a multimegajoule electrical energy source, such as an explosive generator, to plasma kinetic energy, and that high implosion speeds (> 30 cm/μsec) can be obtained so that hydrodynamic times are short. For plasma kinetic energies in the MJ range and hydrodynamic times of 10^{-8} sec, the radiation power is of the order of 10^{14} watts.

A difficulty frequently encountered when attempting to heat a plasma by a high current discharge arises from the decrease in ohmic heating, because of the rapid increase in electrical conductivity of a plasma at high temperatures, coupled with a rapid increase in radiative cooling. A moving discharge can have

a substantial dissipative impedance regardless of its temperature as the following analysis will show.

If the resistance of the plasma can be neglected, the voltage drop across the discharge, V, equals the rate of change of the flux in the discharge.

$$V = \dot{\phi}_D = \frac{d}{dt}(L_D J) = L_D \dot{J} + \dot{L}_D J \tag{1}$$

ϕ_D is total magnetic flux in the discharge volume, L_D is the inductance, and J is the axial current. L_D is the usual inductive reactance, relating the voltage to the rate of change of the current, L_D gives a voltage drop similar to that arising from a resistance since L_D is increasing; however, it is not a loss term since it is proportional to the foil velocity. The power, P_D, going into the discharge is obtained by multiplying both sides of this equation by the current.

$$P_D = L_D J \dot{J} + \dot{L}_D J^2 \tag{2}$$

Part of this power input leads to radially directed plasma kinetic energy, and the rest to magnetic field energy in the volume around the discharge. The magnetic energy at any time t is given by $1/2\ L_D J^2$. Differentiating, the power input to the magnetic field, P_M, is

$$P_M = L_D J \dot{J} + 1/2\ \dot{L}_D J^2 \tag{3}$$

The first term arises from the change in the magnetic field intensity, and the second term arises from the change in the volume occupied by that field. The input to the plasma kinetic energy, P_K, is therefore

$$P_K = 1/2\ \dot{L}_D J^2 \tag{4}$$

This relation can be derived directly by considering the work done on the plasma. To complete the link between the impedance and power expressions and the plasma dynamics, we can write

$$L_D = \frac{\mu_o}{2\pi} h\ \ell n\ [R_o/r(t)] \tag{5}$$

$$\dot{L}_D = \frac{\mu_o}{2\pi} h\ [v(t)/r(t)] \tag{6}$$

Here, h is the height of the cylindrical discharge, r(t) is the radius, v(t) is the implosion speed, R_0 is the radius of the outer conductor (the current return), and $\mu_0 = 4\pi \times 10^{-7}$ H/m.

Two items of major interest are the efficiency of energy transfer from the power source to the plasma and the maximum radial velocity of the plasma. The question arises as to what general statements can be made concerning the power supply which will optimize the above quantities. Ordinary maximum power transfer conditions would require that the power supply impedance match the discharge impedance. Unfortunately, both impedances vary considerably during the plasma implosion. Moreover, energy fed into the discharge inductance early in the run will reappear later as plasma kinetic energy through the $\vec{j} \times \vec{B}$ forces. This energy will not go back into the generator if it has a sufficiently low inductance at later times. Detailed numerical calculations are necessary to set requirements on the power supply. About all that can be said at this point is that the necessary energy must be available and that it must be transferred to the discharge in a time comparable to that required for the plasma to implode at an average velocity of some tens of cm/μsec. For the systems considered here, this time is of the order of 1 to 2 μsec.

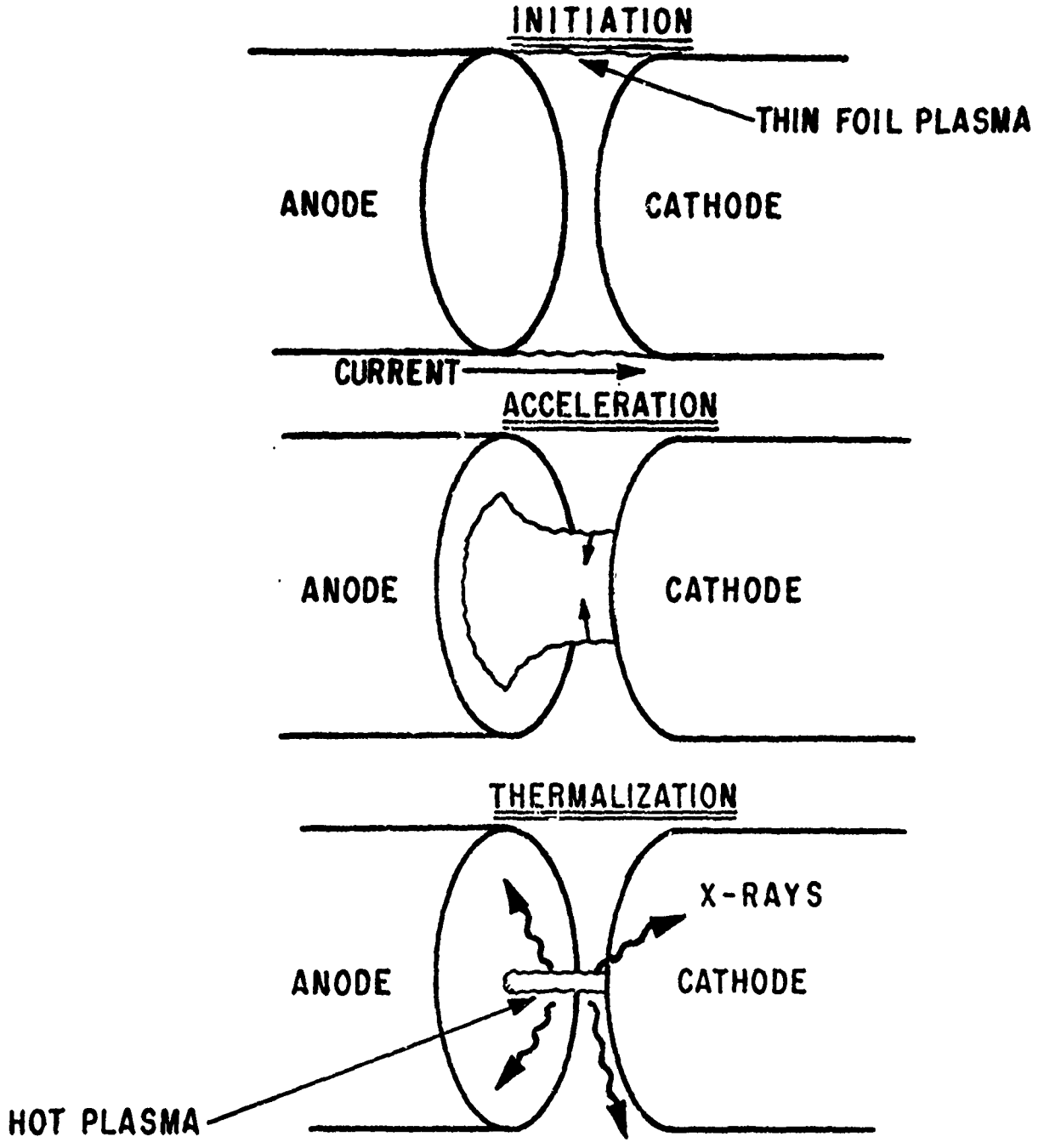

Figure 1. Schematic representation of the initiation, acceleration, and thermalization phases of the EM implosion. For the sake of clarity, the cylindrical return conductor on the outside of the system is not shown

SECTION III

EXPLOSIVE GENERATORS

In an explosive generator an initial amount of electrical energy is stored in an inductor which is then explosively compressed (ref. 2). Conservation of magnetic flux in a situation of rapidly decreasing inductance requires a corresponding increase in current by a factor approximately equal to the ratio of initial to final inductance. In changing the inductance, work is expended at a rate $1/2\ \dot{L}_G J^2$, where L_G is the generator inductance. In this way, the chemical energy of the explosive is converted to electrical energy. Since 1 kilogram of high explosive is equivalent to about 5 megajoules of energy, explosive generators can in principle be extremely compact multimegajoule sources of electrical energy.

The equivalent circuit of a generator operating into a noncapacitive load is shown in figure 2. The basic equation governing the behavior of the generator in such a circuit is given by summing the emf's around the loop.

$$\dot{L}J + L\dot{J} + RJ = 0 \tag{7}$$

Here, $L = L_G + L_1$, and all the circuit parameters are to be regarded as functions of time. Rearranging the terms and integrating, the following solution is obtained:

$$J(t) = \frac{J_0 L_0}{L(t)} \exp\left[-\int_0^t \frac{R(\tau)}{L(\tau)}\, d\tau\right] \tag{8}$$

J_0 and L_0 are the initial values of the current and the total circuit inductance, respectively. It is assumed that generator action starts at $t = 0$

If the inductance is a monotonic function of time, the exponential term may be rewritten

$$\int_0^t \frac{R(\tau)}{L(\tau)}\, dt = \int_{L_0}^{L} \frac{R(t)}{\dot{L}(t)} \frac{dL}{L} \tag{9}$$

$R(t)$ may be constant or a fairly complex function of time. However, for the sake of simplifying the discussion, assume that $R(t)/\dot{L}(t) = -k$, where k is a positive constant. The current equation becomes

$$J(t) = J_0\left[\frac{L_0}{L(t)}\right]^{1-k} \tag{10}$$

For current multiplication, k must be less than 1, or $R(t) < -\dot{L}(t)$. The corresponding expression for the energy output is

$$E = \mathcal{E}_0\left[\frac{L_0}{L(t)}\right]^{1-2k} \tag{11}$$

Thus, for energy gain, $R(t) < -1/2\,\dot{L}(t)$. From this simple analysis it is clear that, in general, two conditions must hold over the time when most of the energy is transferred. The first is that the total circuit inductance must decrease and the second is that $R(t) < 1/2\,|\dot{L}(t)|$. Generally, the resistance and $\dot{L}_G$ of the generator will both be proportional to distance along the current path so that their relative values will depend on other aspects of generator geometry and on the properties of the conductor material. In later sections, resistive losses will be considered in detail. For the load impedances of interest here, the explosive generator equivalent impedance, $\dot{L}_G$, should exceed ohmic resistance by about a factor of ten or more. Therefore, in the numerical computations presented in section 4, series resistance has been ignored. The validity then will be examined in view of resistive loss, thermal loading, and other experimental factors.

There are many generator designs described in the literature for a wide variety of applications. However, the requirements in the present case are for the delivery of around 5 MJ in 2 μsec or less with a peak current in excess of 50 MA. A great many of the existing designs can be excluded immediately from consideration as being too slow. The power output implied is greater than 2.5 TW, and the only way this output can be produced is to have a large area of conductor doing work against a high magnetic field. There are two basic techniques for achieving this result. One involves the initiation of the explosive in a simple way at a point or along a line on the surface. The conductor then is machined into a shape which ensures simultaneous arrival at some opposing surface. In addition to requiring an extensive experimental and computational program to arrive at the correct shape, the machining costs often turn out to be very high even with the modern tape-controlled equipment. The other technique is to employ a simple conductor shape but to initiate the explosive simultaneously over a large area. The availability and relatively low cost of good plane initiation systems

was the deciding factor in the choice of the plate and disc generators for the percent feasibility study. The plane systems make it possible to proceed with a development program aimed at imploding plasma experiments within a reasonable length of time. Later, if a higher energy generator seems desirable, it may be worthwhile to look more closely at other configurations.

The basic geometries of the two generator designs are shown in figures 3 and 4. The first is termed (somewhat arbitrarily) a plate generator. It is essentially a parallel plate transmission line with rectangular explosive slabs on the two current-carrying conductors. When the explosive is detonated simultaneously over the outer surfaces, the resulting plane detonation front drives the two plates together, decreasing the inductance. This type of generator has been described in references 3, 4, and 5.

The disc generator of figure 4 has not been described before to the best of the authors' knowledge. It consists essentially of a short coaxial transmission line in which the ends are driven together by discs of explosive. It should be noted that some design precautions are necessary to prevent the explosive from shorting the inner and outer conductors together before the disc can finish its run. The annular space can be increased in the region opposite the explosive, for instance. In addition, since the current would be confined to a narrow region at the outer radius of the inner conductor, it would be possible to use several layers of alternating low and high density materials to slow down the radial motion. Finally, the thickness of the disc should be tapered in such a way as to ensure that the portion near the central rod would reach the midplane before the region near the outer conductor.

Referring to figures 3 and 4, the relevant inductance formulas follow.

Plate generator:

$$L_G = \mu_0 \frac{\ell}{w} x \tag{12}$$

$$\dot{L}_G = \mu_0 \frac{\ell}{w} v \tag{13}$$

Disc generator:

$$L_G = \frac{\mu_0}{2\pi} x \ln\left(\frac{R_2}{R_1}\right) \tag{14}$$

$$\dot{L}_G = \frac{\mu_0}{2\pi} v \ln\left(\frac{R_2}{R_1}\right) \tag{15}$$

It is assumed in the following analysis that the velocity of the plates or discs is constant over the run. This approximation is sufficiently accurate for the present work.

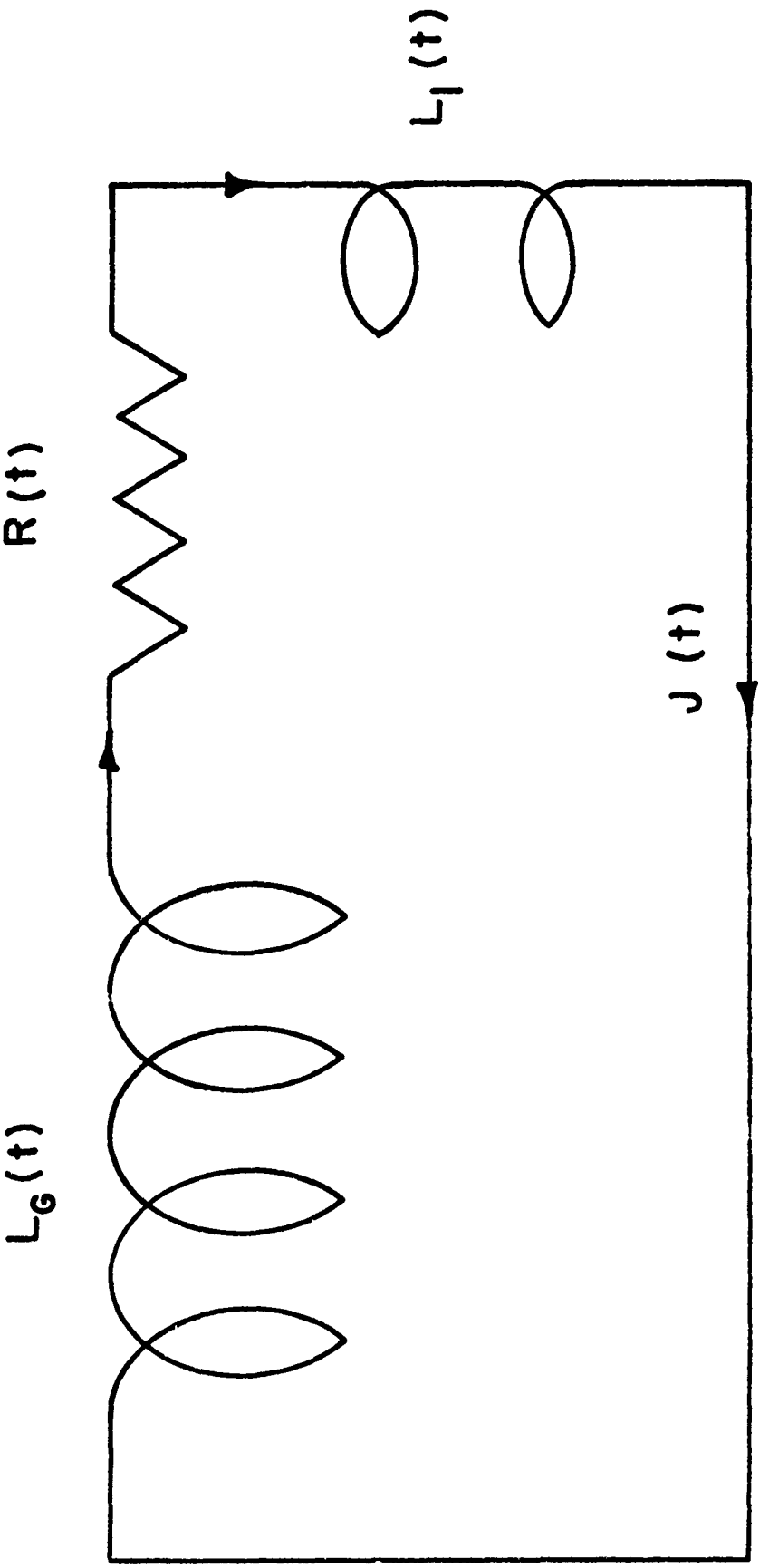

Figure 2. Equivalent circuit of an explosive generator operating into a noncapacitive load

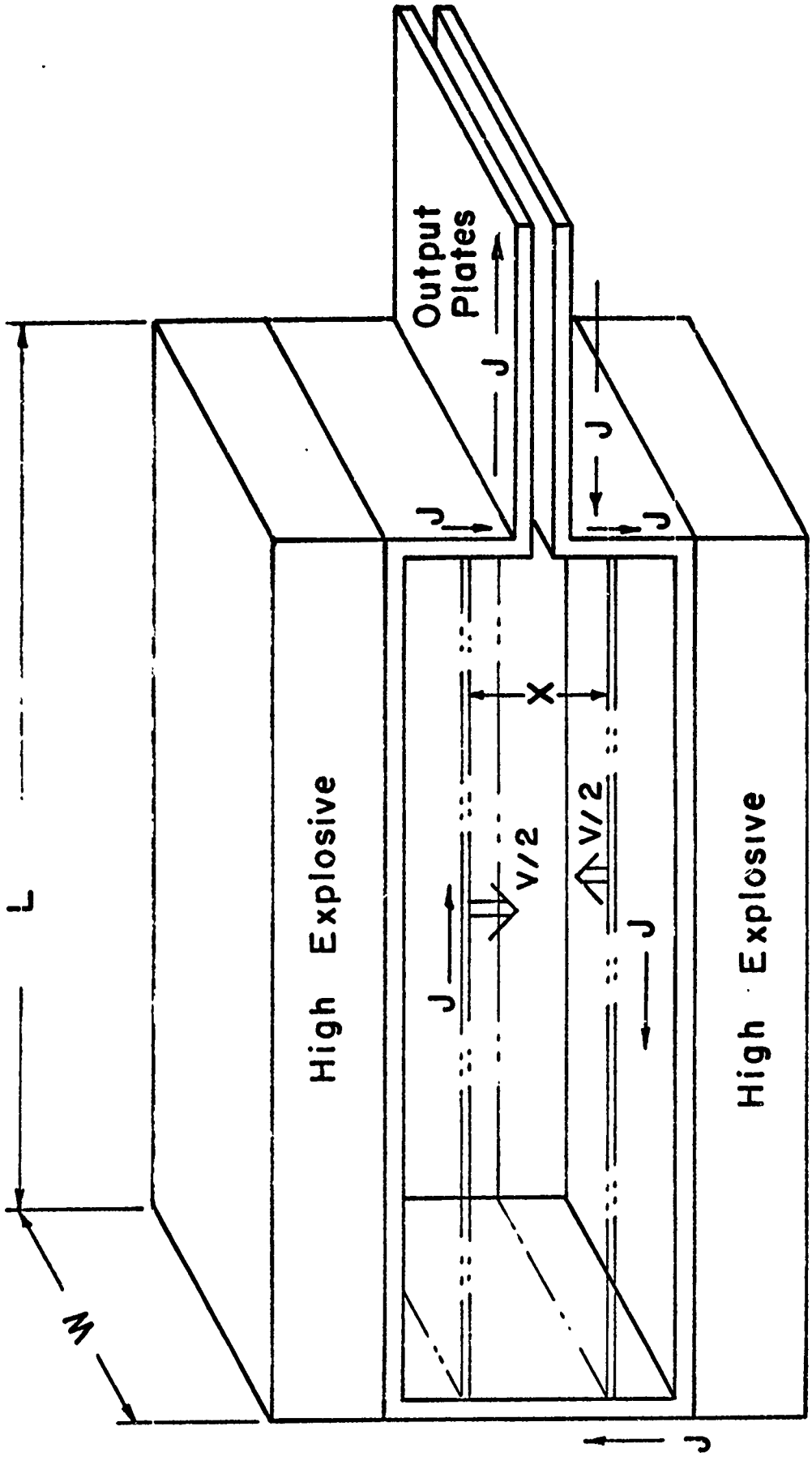

Figure 3. Schematic representation of a plate generator. The input system for obtaining the initial flux is not shown

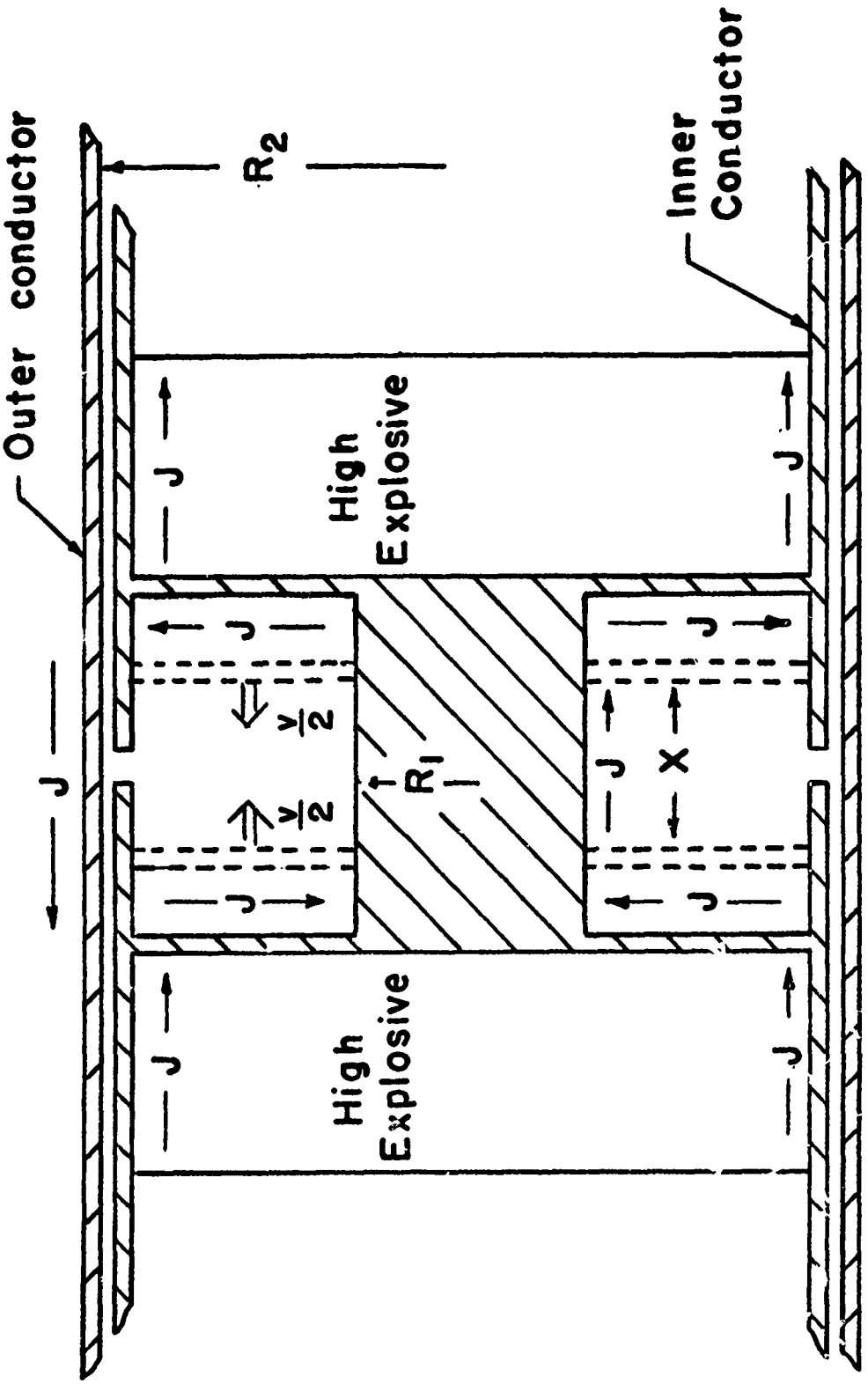

Figure 4. Schematic representation of a disc generator

SECTION IV

NUMERICAL CALCULATIONS

Since the coupling of the dynamic plasma discharge and the explosive generator must be strong to obtain high energy transfer efficiencies, the governing set of equations is nonlinear and exact analysis requires numerical computation. To arrive at a regime of interest to which detailed qualitative discussion could be directed, parametric studies were performed in which the set of equations governing the circuit shown in figure 5 is solved for various circuit values. A general time-varying (decreasing) inductor is taken to represent the generator while another time-varying (increasing) inductor is used to express the dynamic plasma impedance.

Energy is initially stored in the inductance of the left-hand side of the circuit, with current flowing through a dummy or parallel load, L_p, prior to switching in the EM implosion load, L_D. The purpose of the dummy load and switch is to keep the current out of the foil during the early slow rise of the generator output, while permitting current to flow in the generator. It is a technique for increasing the risetime of the current in the load without appreciably affecting the final energy transferred. In the results presented, the initial electrical energy of the system is 300 kJ (provided for example by a capacitor bank). The initial foil thickness is kept constant in these calculations at 1.0 μm, and the foil material is aluminum. The generator inductance is assumed to decrease linearly, reaching a minimum inductance of 1.0 nH (L_M) in a time given by the interconductor gap in the generator divided by the gap closure speed. Typical generator times in the systems considered are a few microseconds, and switching occurs instantaneously at some time during generator operation (expressed as a fraction of the total generator time). For example, in figure 6, the generator current and discharge current are shown versus time after switching, which occurs in this case with 20 percent of generator operation remaining. The initial generator inductance is 55 nH with L_p = 10 nH, and the total generator operating time is 4.75 μsec. The sharp peaks in current indicate completion of the generator run, with the subsequent sharp decrease due to the increasing inductance of the discharge as the foil continues to move inward. In this case, the initial foil

radius is 10 cm and the foil height, 1 cm. The radius and velocity of the implosion are shown in figure 7.

Results obtained by coupling the same generator to various EM implosion loads are presented in figures 8 and 9. Here, the initial radius of the foil is varied. With an initial generator inductance of 55 nH and switching the generator into the load after 80 percent of its total run (3.75 μsec), implosion speeds in excess of 50 cm/μsec and efficiencies of about 50 percent are calculated. Efficiency in the cases presented is defined as final plasma kinetic energy divided by initial energy plus electrical energy delivered to L_p and the discharge at the time of final plasma collapse. For this particular generator, plasma kinetic energies, E_K, up to 3 MJ may be obtained with high implosion speeds.

The importance of proper timing is shown in figure 10, where efficiency and final foil speed are plotted against the time of switching to the load (expressed as a fraction of the generator run time). The results obtained are for an initial foil radius of 10 cm driven by the same generator used to obtain the results in figure 6. The dependence of efficiency on timing may be seen more generally in figure 11 in which efficiency is plotted versus the power delivery time divided by the implosion or pinch time for several initial foil radii and a range of switch times. The power delivery time is the generator run time remaining after switching in the dynamic plasma load. The decrease in plasma kinetic energy and efficiency for switch times greater than about 70 percent of the generator run time (figure 10) and also for generator delivery times less than the plasma implosion time (figure 11) arise from influence on the generator circuit of the dummy load L_p. If the switching is delayed until the remaining inductance of the generator is comparable to that of L_p, the current multiplication is significantly lower than would have been the case had the lower impedance-discharge load been in the circuit earlier. Thus, the generator power output ($L_G I^2$) is less after switching occurs. Moreover, a greater proportion of the generator energy is left in L_p, lowering the efficiency. This situation can be corrected to some extent by lowering the value of L_p; however, when the impedance of L_p becomes comparable to that of the discharge circuit, a disproportionately large share of the generator output will go to L_p. The decrease in efficiency for power delivery times greater than the pinch time is caused by the increase in discharge inductance during the early part of the generator run. The generator output current does not build up very rapidly after switching because of the higher impedance, and

the energy going into the discharge is less. Generally speaking, the power delivery time should be roughly equal to the pinch time for best performance.

The results of calculations for higher initial inductance systems are shown in figures 12 and 13. The initial energy supplied is maintained at 300 kJ, switching occurs after 60 percent of the generator run and a 12 cm initial radius foil is used. From these calculations, it appears that implosion speeds in excess of 100 cm/μsec and plasma energies approaching 20 MJ may be obtained, with efficiencies of 60 percent. These analyses only indicate that it is electrodynamically possible to transfer large amounts of energy efficiently to dynamic loads characteristic of cylindrical plasmas imploding at high speed.

To establish the feasibility of operating explosive generators in this regime of current, energy and pulse time, it is necessary to consider generator behavior in greater detail.

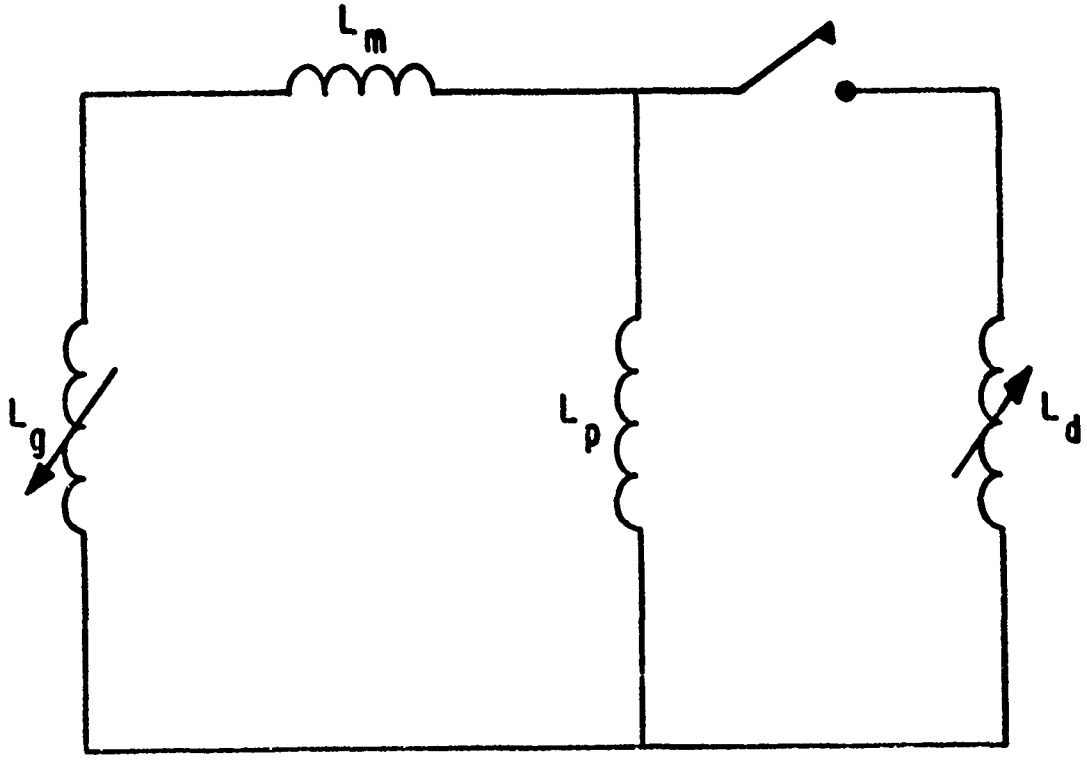

Figure 5. Equivalent circuit used in the numerical calculations of the generator driven EM implosion

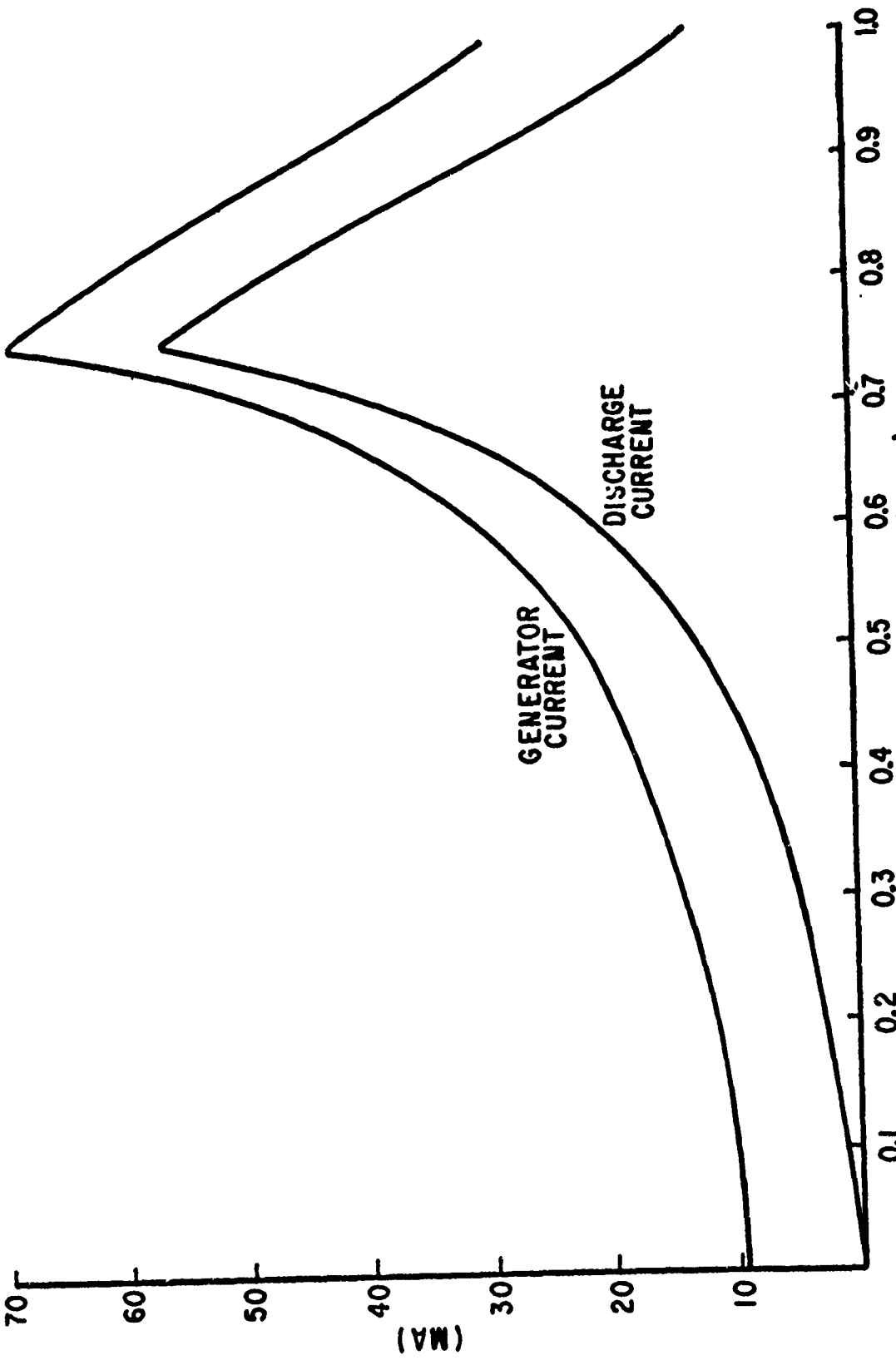

Figure 6. Generator current and discharge current versus time. The origin of the time axis is taken as the time of switch closure, which occurs in this case with 20 percent of generator operation remaining. The initial generator inductance was 55 nH, and L_p was equal to 10 nH. The initial foil radius and height were 10 cm and 1 cm, respectively

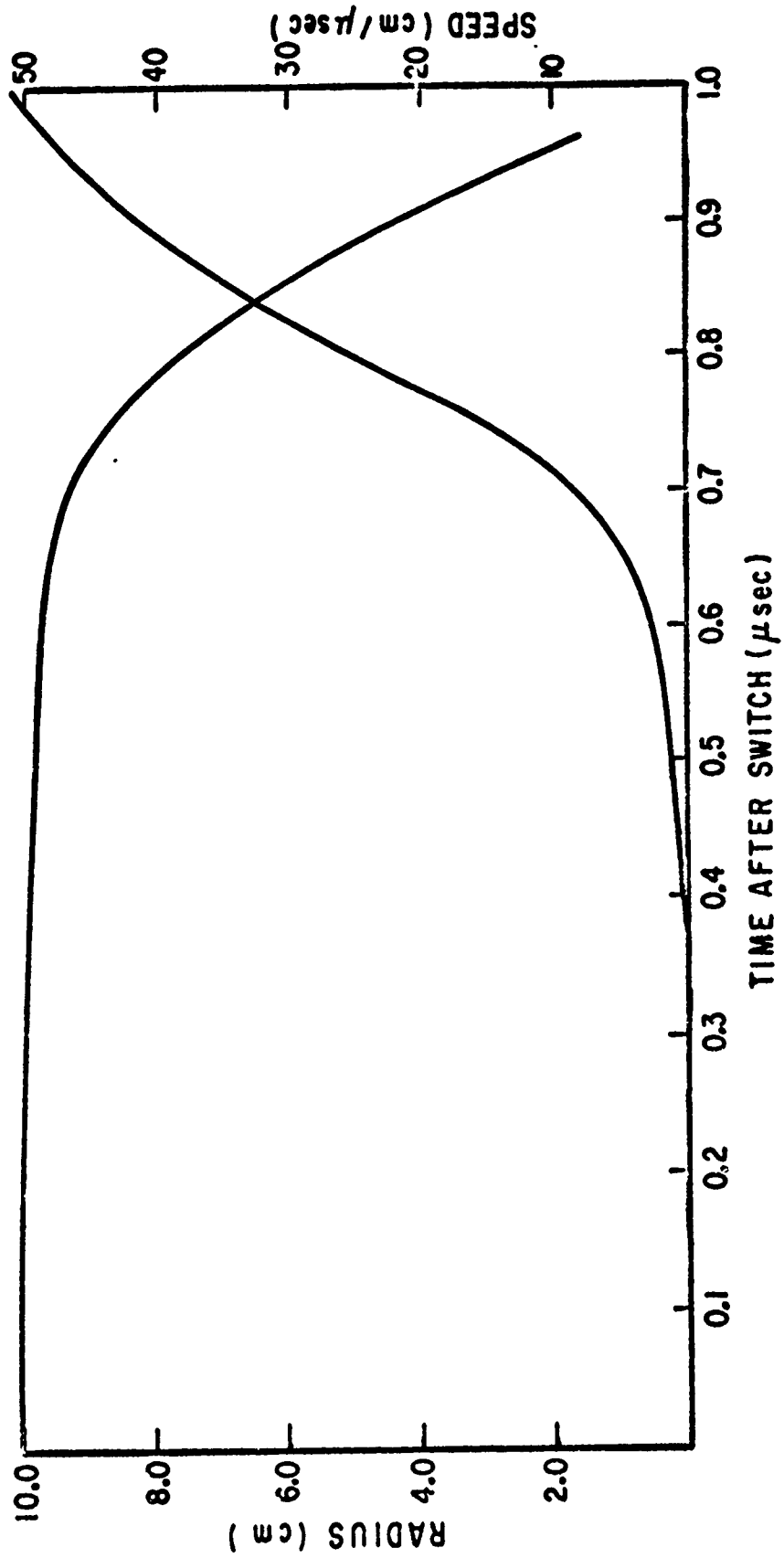

Figure 7. Foil plasma radius and velocity versus time. The problem parameters are the same as those used for figure 6

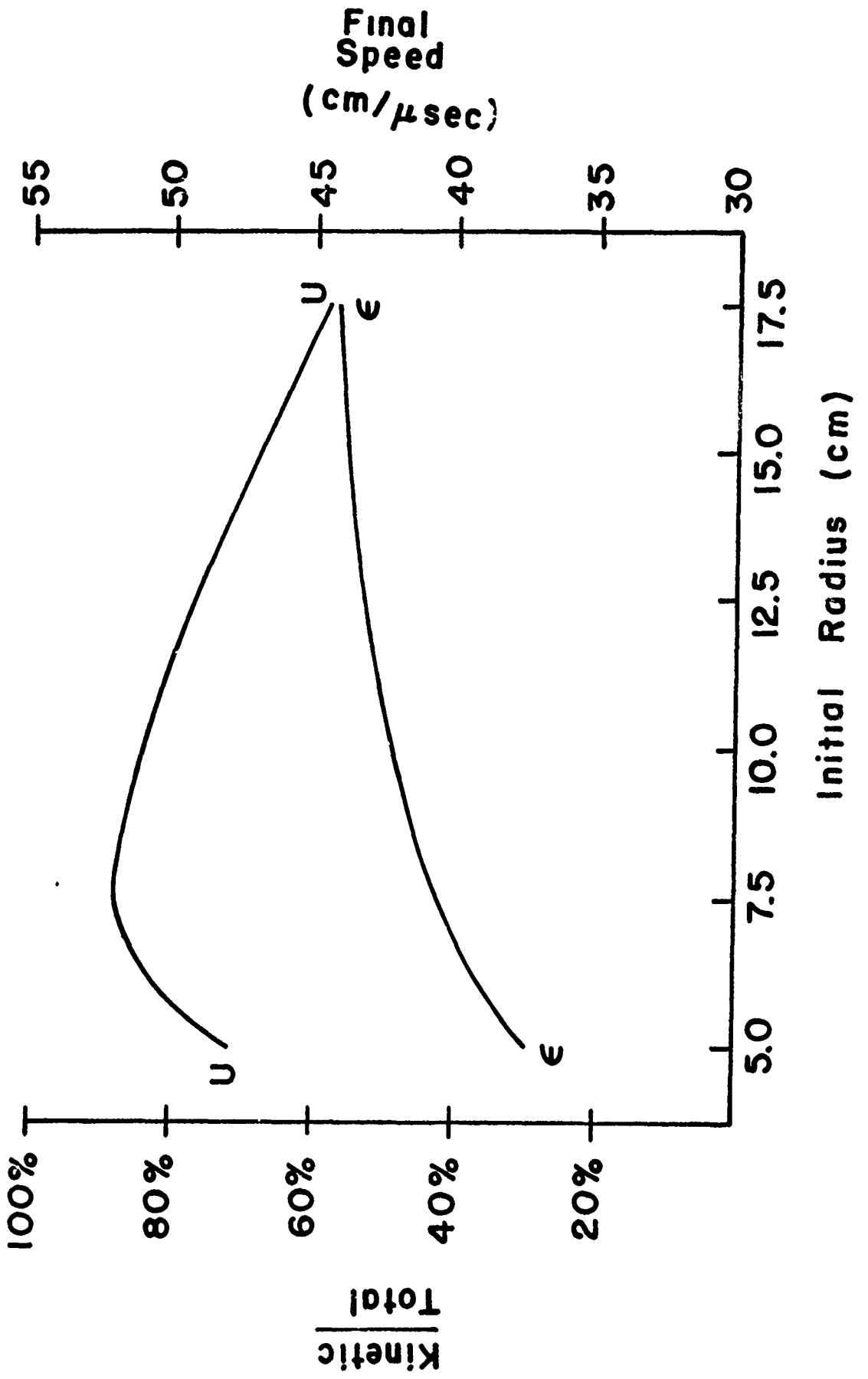

Figure 8. Efficiency (ε) and final velocity (U) of the foil plasma versus initial foil radius. The generator and switching parameters are the same as those used for figure 6

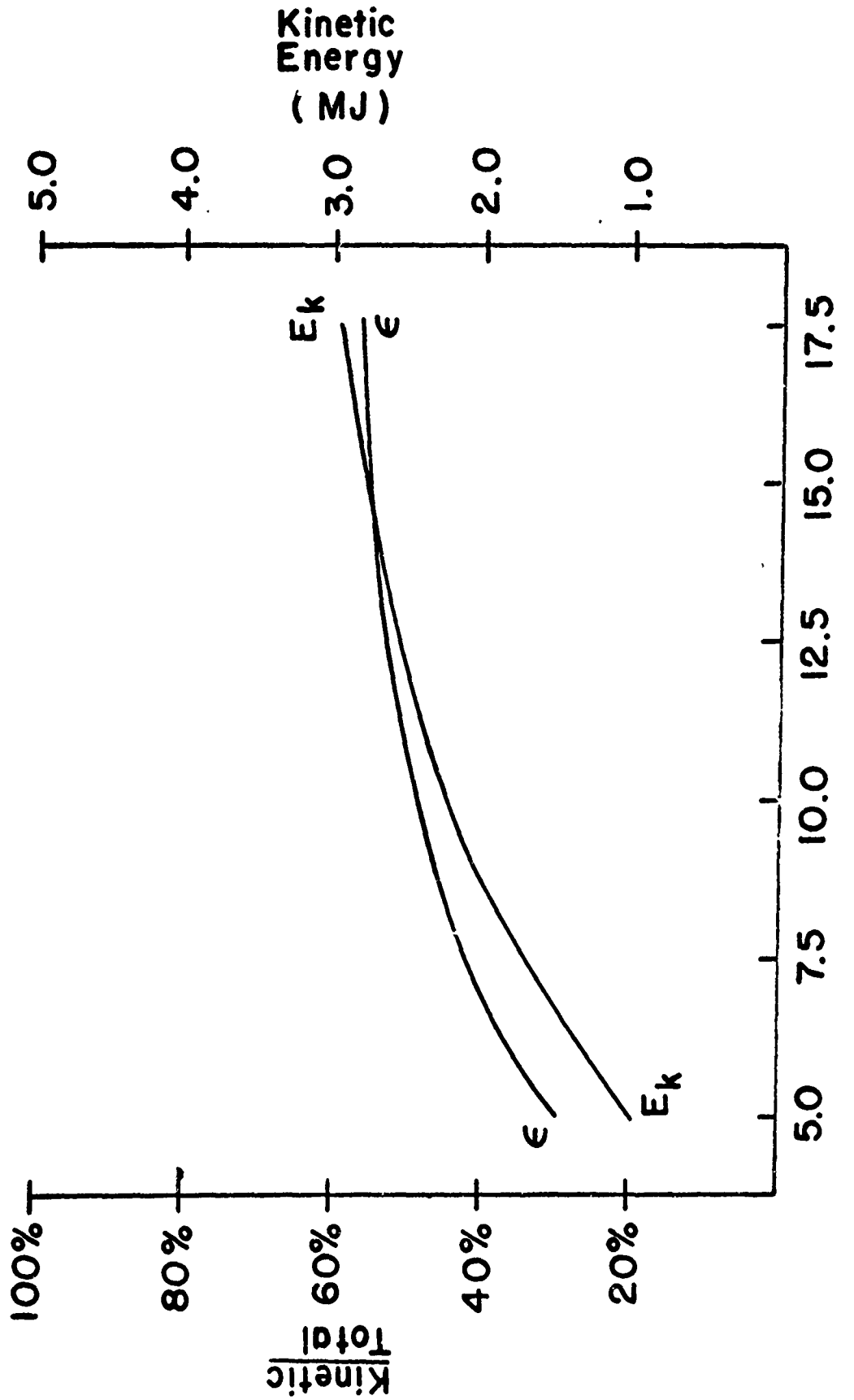

Figure 9. Efficiency (ϵ) and final kinetic energy (E_K) of the foil plasma versus initial foil radius. The generator and switching parameters are the same as those used for figure 6

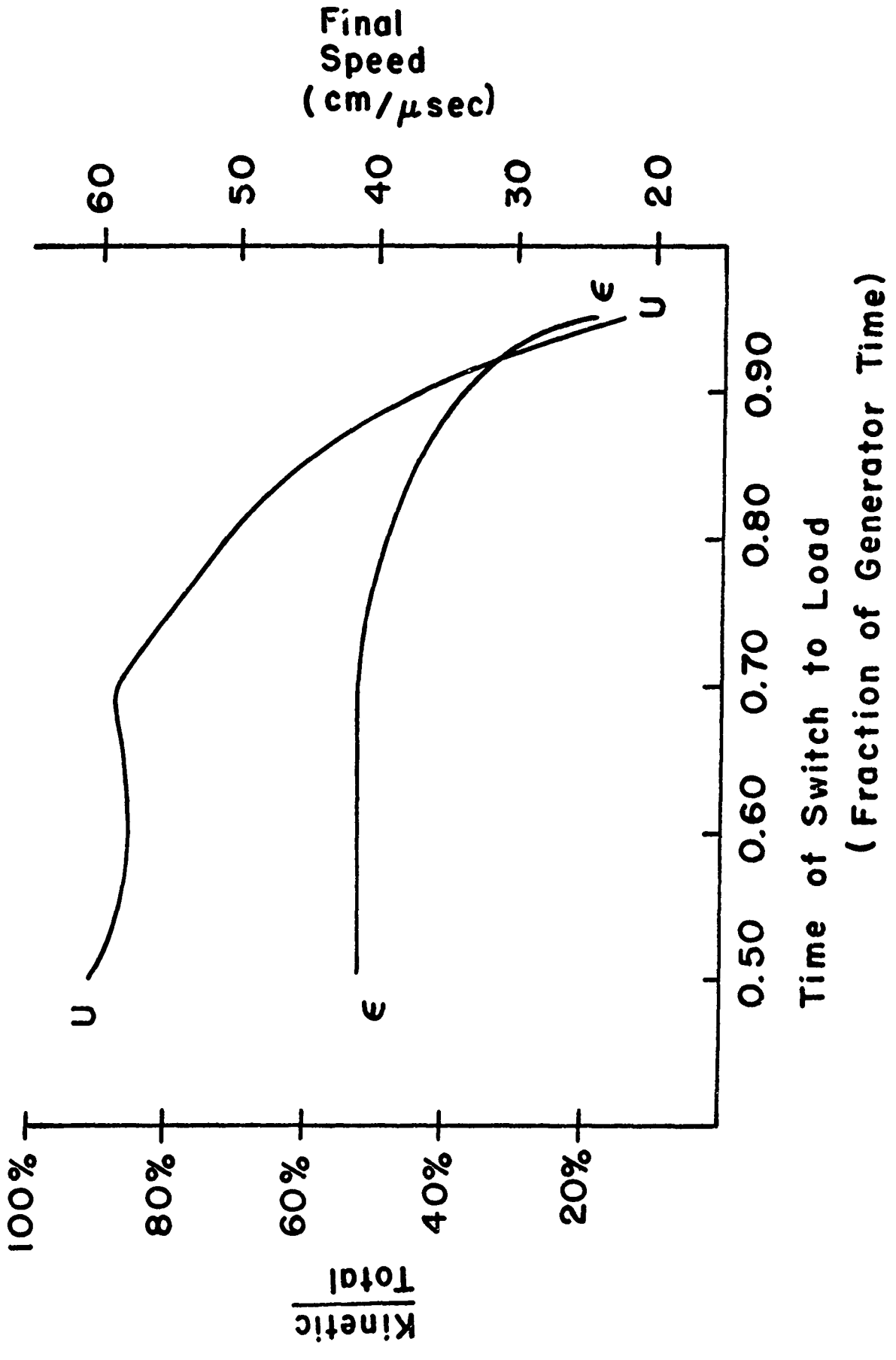

Figure 10. Efficiency (ε) and final velocity (U) of the foil plasma plotted against the fraction of the total generator time elapsed when the switch is closed. The other problem parameters are the same as those used for figure 6

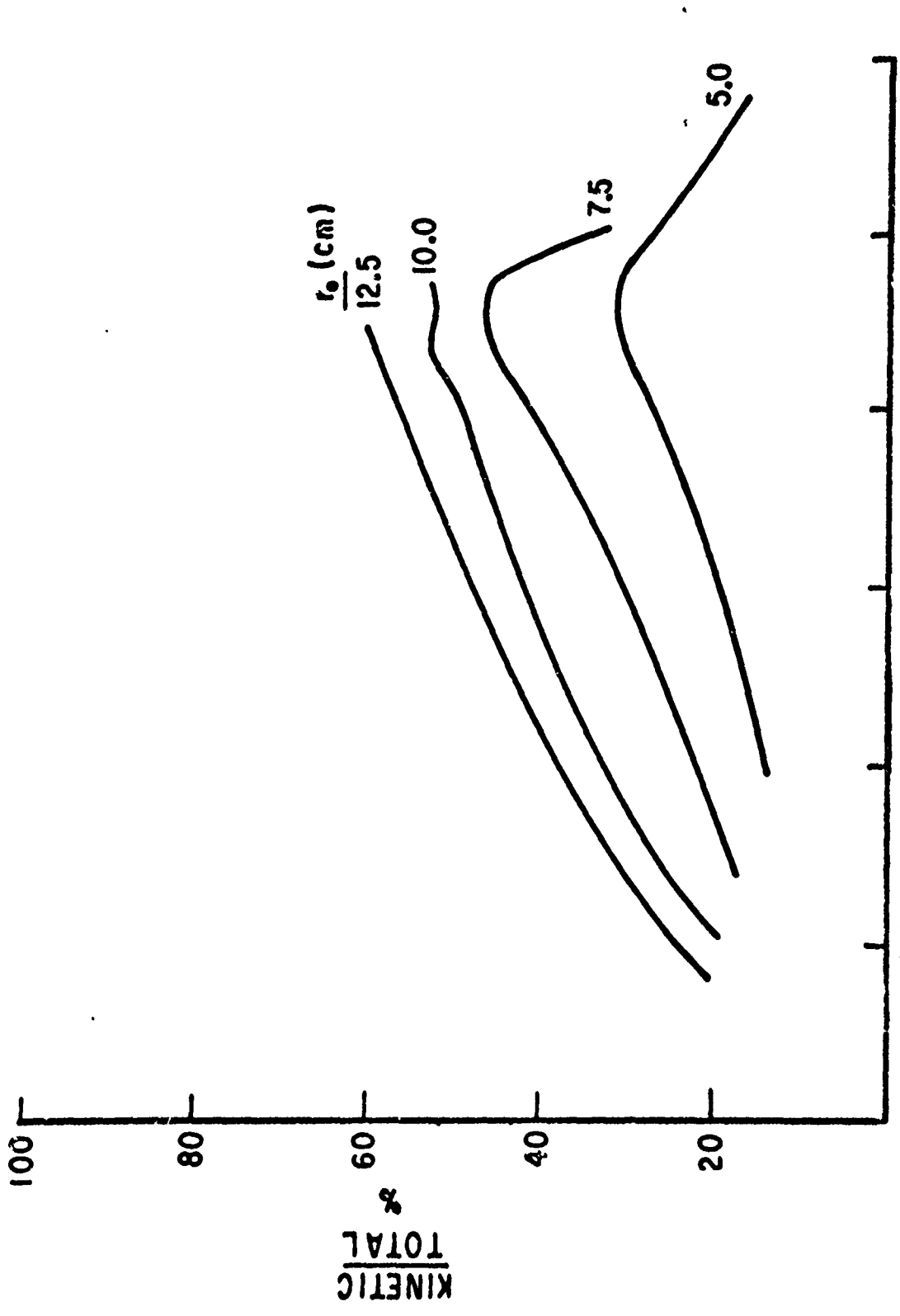

Figure 11. Efficiency of energy delivery as a function of the ratio of power delivery time to pinch time for several foil initial radii. The generator parameters are the same as those used for figure 6

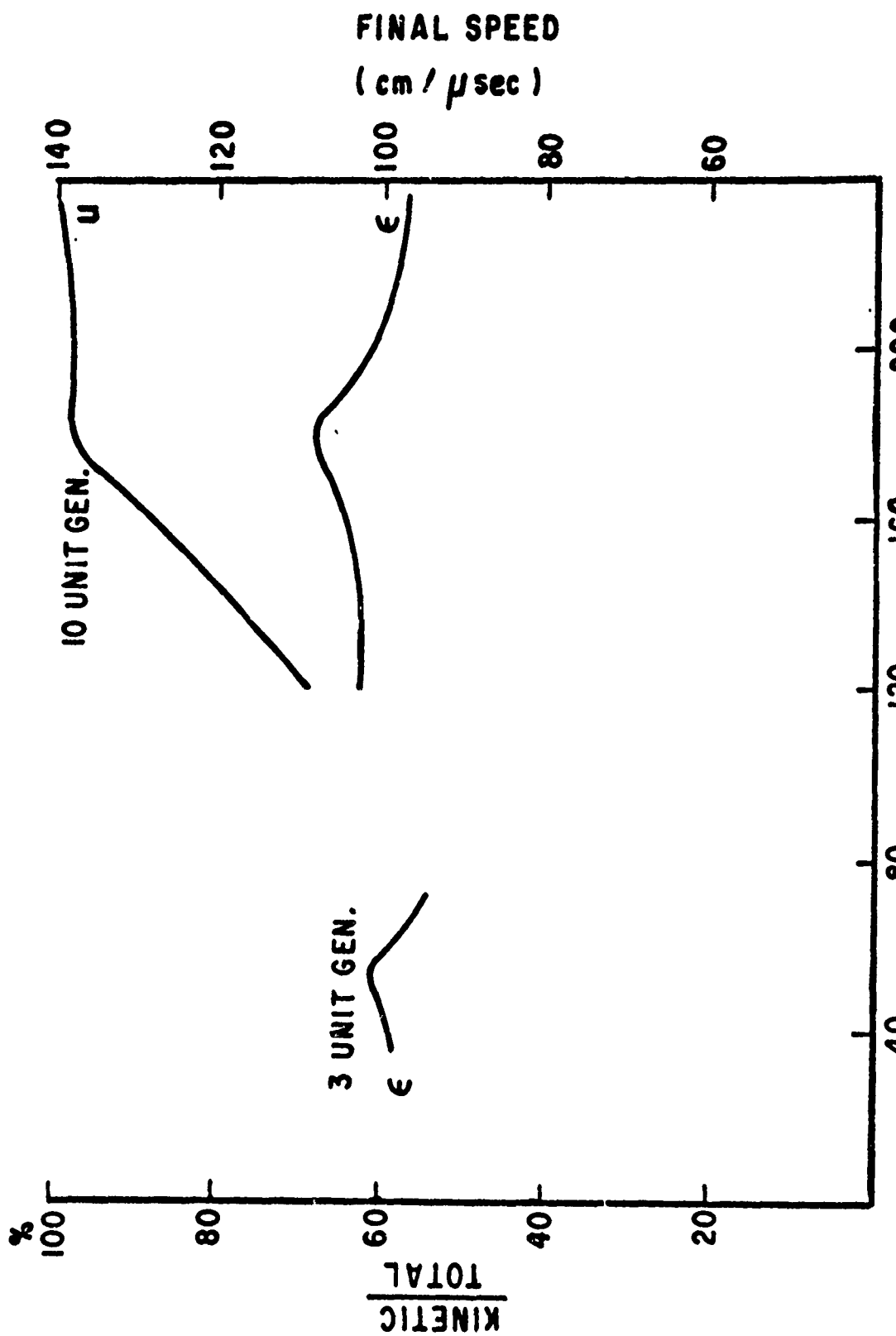

Figure 12. Efficiency (ε) and final plasma velocity (U) versus generator initial inductance. Initial energy is still 300 kJ and switching occurs after 60 percent of the generator run time has elapsed. In initial foil radius is 12 cm

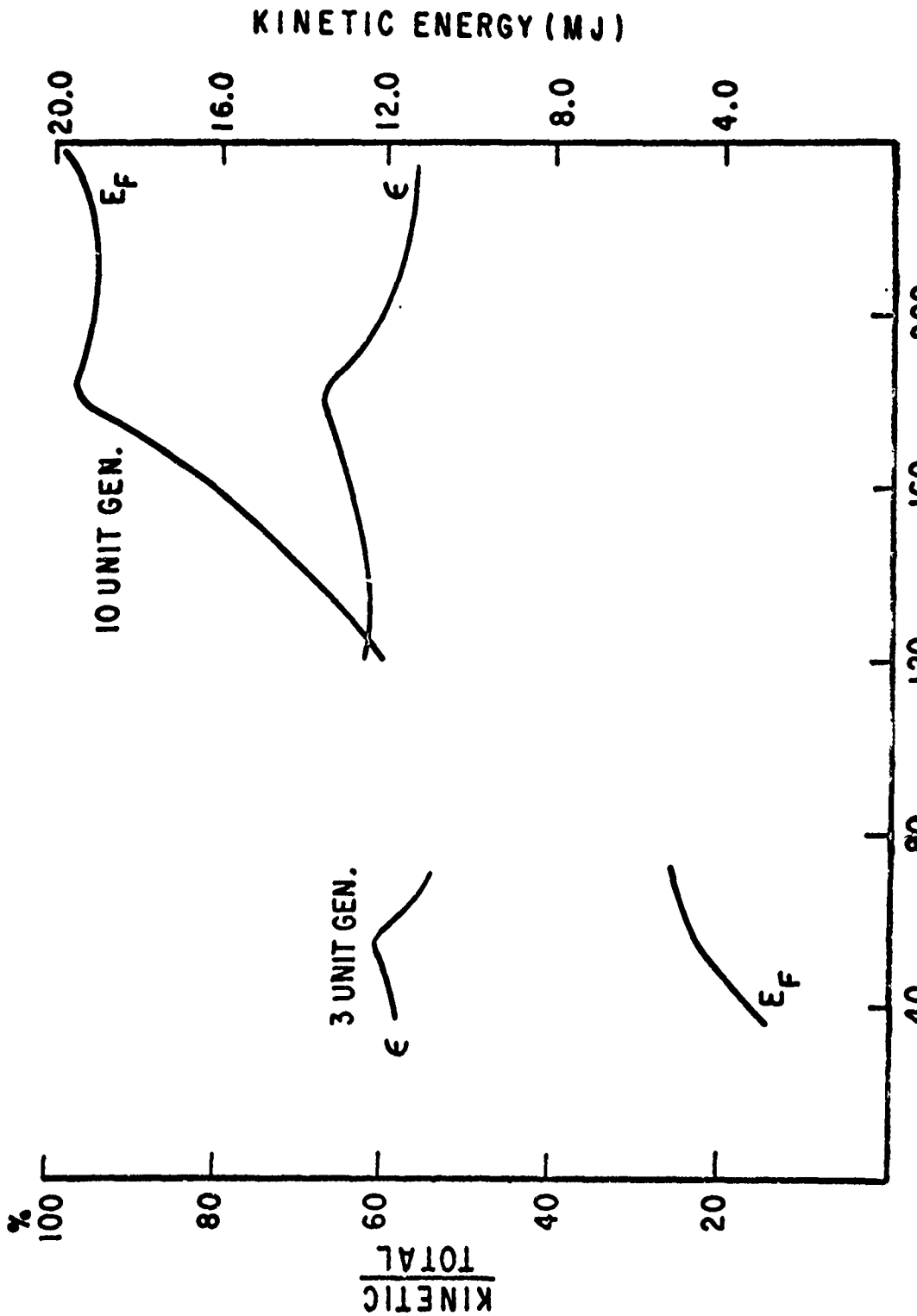

Figure 13. Efficiency (ϵ) and final plasma kinetic energy (E_F) versus initial generator inductance. The other parameters are the same as those given for figure 12

SECTION V

HIGH VOLTAGES

The desired values of energy ($\sim$ 5 MJ), current ($\sim$ 50 MA) and pulse time ($\sim$ 2 μsec) combine to require high voltages somewhere and at some time in generator operation. The expected voltages can be estimated from the expression for the power, i.e.,

$$E_G/\tau = JV_D \; ; \; V_D = 50 \text{ kV} \tag{16}$$

where E_G is the generator energy and τ is the pulse time.

In figure 14, the voltage across the parallel inductor, Lp, is plotted versus time for the same generator conditions whose results are presented in figures 6 and 7. The first sharp rise in voltage is due to the increase in discharge current before the dynamic load has developed much velocity, $V \cong L_D\dot{J}_D$. The sudden drop in voltage at 0.75 μsec occurs because the generator run terminates at this time and $\dot{L}_G$ is zero thereafter. After this time the plasma is being driven by the stored magnetic field. The second sharp increase in voltage occurs during the final stage of plasma collapse when the $L_D\dot{J}$ term, proportional to collapse speed divided by radius, increases rapidly. While it appears that voltages of a few hundred kilovolts are indeed generated, values in excess of 100 kV are attained only slightly before completion of the generator run and peak values exist only for very short times (< 50 nsec). Thus, high voltages associated with high power, high current explosive generator operation may not be a problem when such generators are coupled to EM implosions.

To increase the possibility of operating explosive generator systems without internal arcing, it would be useful to include an electronegative gas (such as sulpher hexafluoride) in the interconductor gap. Operation on the high pressure side of the Paschen curve will be maintained during the explosive compression of the gap so that arcing and surface flashover should be inhibited. Inclusion of very thin sheets of Mylar of polyethylene midway between the conductors should also help to prevent arcing.

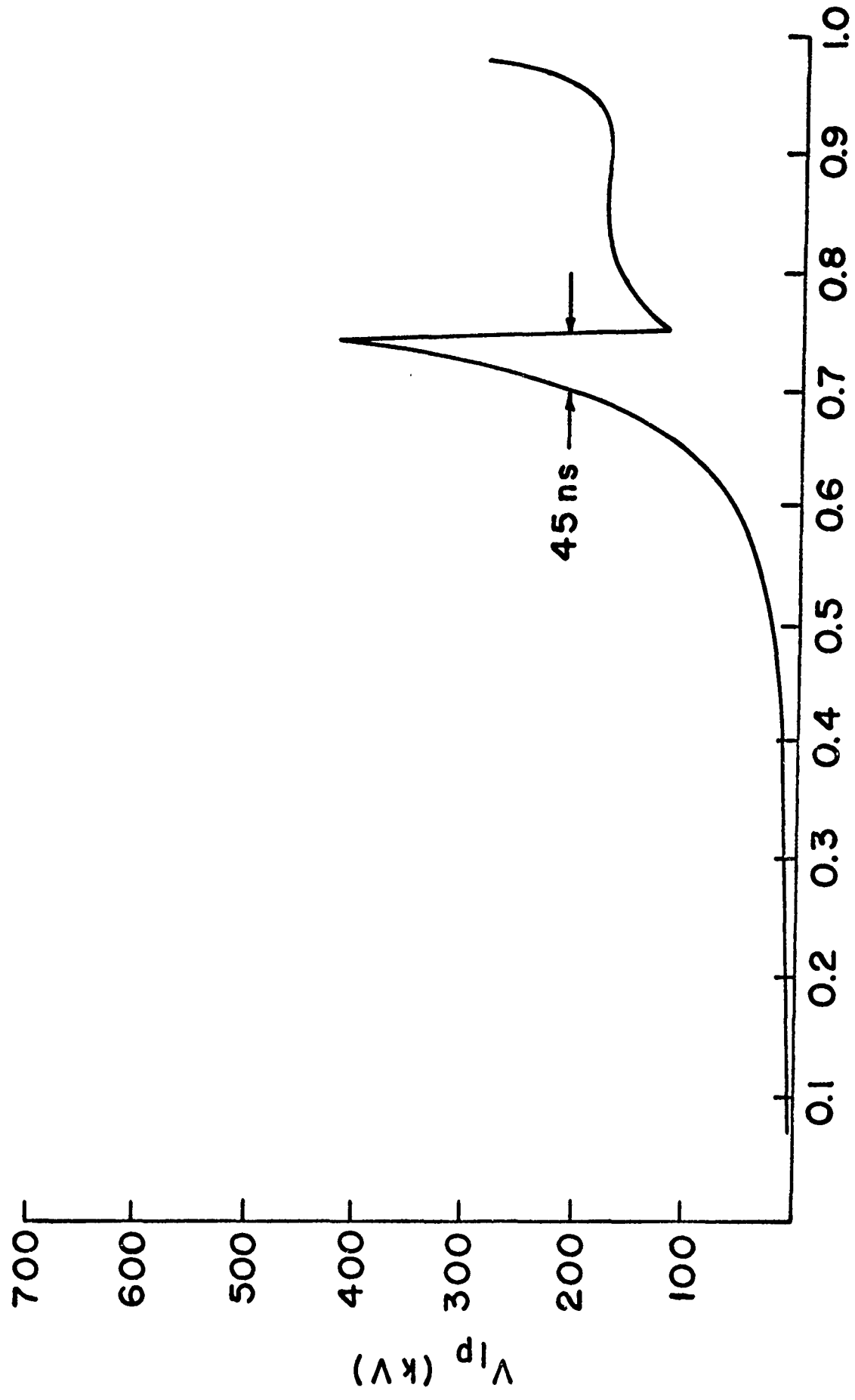

Figure 14. Voltage across the parallel inductor (Lp in figure 5) versus time (after switching) for the problem parameters of figure 6. The abrupt drop in voltage at 0.75 μsec occurs because the generator run terminates at that time and L_G drops to zero

SECTION VI

RESISTIVE LOSSES IN THE GENERATOR

There are two ways in which finite conductivity in the generator can affect the performance. First, the resistive impedance lowers the current at any given stage of the generator action. The effect is more than a mere loss of some of the available output energy to resistive heating. Since the power output at any time depends upon the field and therefore current for the moving conductors to work against, the effect is cumulative and in fact exponential. Referring back to equations 10, 12, and 14 and figure 2 and assuming that $R(t)$ and $L_1(t)$ are constants with time, a simplified solution is obtained which shows the effect of resistance on the current multiplication. The generator inductance is taken to be $L_G = L_0(1-t/\tau)$. Thus, the initial inductance of the total circuit is $L_0 + L_1$, and at generator burnout time, $t = \tau$, only the load inductance, L_1, remains in the circuit. The equations become

$$\frac{J(t)}{J_0} = \alpha_0^{1-k}[F(t)]^{k-1} \tag{17}$$

where $\alpha_0 = 1 + L_0/L_1$ and represents the maximum multiplication obtainable in the absence of resistance.

$$F(t) = \alpha_0 - \frac{t}{\tau}(\alpha_0 - 1) \tag{18}$$

$$\tau = x_0/v_0 = -L_0/\dot{L} \tag{19}$$

$$k = \frac{R\tau}{L_0} = \frac{-R}{\dot{L}} \tag{20}$$

L_0 is the initial generator inductance.

The energy multiplication is

$$\alpha_L = \frac{E_L}{E_0} = \alpha_0^{1-2k}[F(t)]^{2k-2} \tag{21}$$

where $E_L = \frac{1}{2} L_1 I^2$. The exponential dependence on k and therefore R is evident.

It is a possible to estimate roughly the effect of a resistivity η for a plate generator by

$$R = \frac{2\eta\ell}{w\delta} \tag{22}$$

Here, ℓ is the lenqth of a single driver plate, w is the width and δ is the skin depth. The skin depth appropriate to a pulse time τ is approximately

$$\delta = (\eta\tau/\mu_0)^{1/2} \tag{23}$$

Then

$$k = R/\dot{L}_G = 2\left(\frac{\eta}{\mu_0 x_0 v_G}\right)^{1/2} = 2/R_M{}^{1/2} \tag{24}$$

where R_M is the magnetic Reynolds number.

At generator burnout time, τ, the function $F(\tau) = 1$, according to equation 18. From equations 17 and 21, the current and energy multiplication ratios at burnout simplify to the following expressions:

$$J(\tau)/J_0 = \alpha_0{}^{1-k}$$

$$\alpha_L = E_L(\tau)/E_0 = \alpha_0{}^{1-2k} \tag{25}$$

As an example that illustrates the degradation of energy multiplication due to resistance, consider a plate generator with the following characteristics: x_0 = 5 cm; v_G = 8 km/sec and η = 30 $\mu\Omega$-cm. From equation 24, $k \cong 0.05$. For $\alpha_0 = 25$, $\alpha_L = 18.3$. Thus the energy multiplication is 73 percent of that which would have been obtained had the generator been lossless. For $\alpha_0 = 50$, $\alpha_L = 34.1$, representing 68 percent of the lossless energy multiplication ratio. These results, based upon a fixed load inductance with no switching, give only a crude estimate of the error involved in neglecting resistance for the case of a moving discharge in the circuit shown in figure 4.

A second source of loss is the magnetic flux which was sunk into the conductors during the generator run. This flux is trapped within the metal and cannot be transferred to the load. This topic is discussed in reference 4. One point of view is to regard the volume occupied by this field as a residual inductance in series with the generator and load. For the parameters given above, δ = 0.1 cm, and the maximum current multiplication obtainable is about 25. A residual inductance of 1 nH is already in the calculations as mentioned previously.

These losses can be offset in practice by designing the generators with a somewhat larger output capability than is indicated by the no-loss assumptions made earlier. This approach can be checked by performing the SHIVA implosion calculations using a resistance in the equivalent circuit.

SECTION VII

THERMAL LOADING OF CONDUCTORS

The energy lost to resistance in the conductors appears in the form of heat. The formula for the fraction of the total generator output which goes into I^2R losses for the case of the plate generator given in the previous section is

$$\frac{E_R}{E_R + E_{L1}} = \frac{2k\left(1 - \alpha_o^{2k-1}\right)}{1 - 2k\alpha_o^{2k-1}} \text{ for } t = \tau$$

If

$$\alpha_T >> 1 \text{ and } k << 1 \tag{26}$$

$$\frac{E_R}{E_R + E_L} \cong 2k = 2R/\dot{L}_G \tag{27}$$

Thus, for 5 MJ delivered to the load, about 500 kJ will go into heating the conductors when k = 0.05.

It is desirable to operate in a thermal loading range which will keep the conductor temperatures below the melting point, and it is necessary to stay below the vaporization point. If we consider that the heat is dumped into a volume $2\,\delta\,w\,\ell$ in a generator, we can calculate the temperature rise from

$$\Delta T = \frac{E_R}{2w\ell\delta C\rho} \cong \frac{k\,E_G}{w\ell\delta C\rho} \text{ , where } E_G = E_R + E_L \tag{28}$$

ΔT is the temperature rise in °K, C is the best capacity per unit mass per °K, and ρ is the mass density. Substituting from equations 23 and 24 for δ and k, we have

$$w\ell \geq \frac{2E_G}{x_o C\rho\Delta T} \tag{29}$$

as the criterion for thermal loading. Taking ΔT as 650°K to reach the melting point of aluminum, ρ as 2.7 gm/cm^3, and C as 0.9 J/°K-gm,

$$\Delta TC\rho \cong 1.6 \times 10^9 J/m^3$$

Thus for a generator output of 5 MJ and an initial plate separation of 5 cm, $w \ell \cong 0.125\ m^2 = 1250\ cm^2$. The width may be determined from $x_0 = 5$ cm and $L_0 = 60$ nH. The configuration is about as long as it is wide, and therefore the width should be about 35 cm for a 5-MJ output. If the explosive is 8 cm thick (4 cm per driver plate), the total weight is about 18.4 kG (40.5 lb). The electrical conversion efficiency implied is about 6 percent. However, it was indicated in the previous section that the generator would have to be made somewhat larger to obtain the necessary multiplication. Therefore, the generator would be somewhat less efficient.

Before leaving this subject, it should be pointed out that the shock and release waves generated in the driver plates by the action of the explosive will cause a significant temperature rise during the early portion of the generator run. Thus, permissible ΔT may be less than 650°. On the other hand, there are techniques for ameliorating the shock heating effects, nor is the melting point a mandatory constraint. Consequently, the analysis will be carried no further, but shock heating should be kept in mind and may indicate a larger area requirement for a specific design.

SECTION VIII

MAGNETIC PRESSURE EFFECTS ON CONDUCTOR DYNAMICS

An additional constraint on conductor geometry, apart from thermal loading, involves retardation of the collapsing conductors by the strong magnetic forces developed at high current levels. Such retardation may prevent attainment of minimum generator inductance and thereby limit generator output. Insofar as the high explosive has accelerated the conductor plate to maximum velocity before the final stage of generator compression, retardation depends on the loss of kinetic energy of the moving plate to the magnetic field. The conducting plate will be completely stopped when the work done against the magnetic field equals the initial kinetic energy of the plate. Thus, equating the kinetic energy per unit area to the work done per unit area, the distance moved by the plate, Δx, can be determined by the equation

$$\frac{\rho}{2}(d)\,U_0^2 = \int_0^{\Delta x} \frac{B^2}{2\mu_0}\,dx \tag{30}$$

Here, d is the thickness of the plate, U_0, its velocity before significant retardation, and B, the magnetic field. The magnetic field increases in response to compression of the inductor:

$$B = \frac{\mu_0 J}{w} + \frac{\mu_0 J_0}{w}\left(\frac{L_0}{L}\right) = \frac{\mu_0 J_0}{w}\,\frac{x_0}{x_0 - x} \tag{31}$$

J_0 is the initial current in the inductor and $(x_0 - x)$ is the interconductor gap being closed from two sides. Substituting,

$$\frac{\rho}{2}\,d\,U_0^2 = \int_0^{\Delta x} \frac{\mu_0 J_0^2}{2w^2}\,\frac{x_0^2}{(x_0 - x)^2}\,dx = \frac{\mu_0 x_0^2 J_0^2}{4w^2}\int_{x_0 - 2\Delta x}^{x_0} \frac{dy}{y^2}$$

$$= \frac{\mu_0 x_0 J_0^2}{2w^2}\,\frac{\Delta x}{(x_0 - 2\Delta x)} \tag{32}$$

$$\Delta x = x_0\left(\frac{\mu_0 x_0 J_0^2}{\rho w^2 x\, u_0^2} + 2\right)^{-1} \tag{33}$$

With $E_0 = 1/2\ L_0 J_0^2 = \frac{\mu_0 x_0 \ell J_0^2}{2w}$, the initial energy provided the inductor, and $E_K = 1/2\ \rho w \ell d U_0$, the initial kinetic energy of the plate,

$$\Delta x = \frac{x_0/2}{(1 + E_0/2E_K)} \tag{34}$$

Thus, the interconductor gap can never be completely closed ($\Delta x = x_0/2$) if the initial magnetic flux is trapped completely within the inductor. Since energy normally flows to an external load, however, complete closure can usually be expected.

The skin effect is, of course, an additional mechanism which prevents the flux from being completely trapped. To allow a qualitative discussion, suppose closure is assumed to be complete when $x_0/2 = \Delta x = \delta$. Then

$$\frac{x_0}{2}\left(\frac{E_0/2E_K}{1 + E_0/2E_K}\right) = \delta \tag{35}$$

$$E_K = \frac{E_0}{2}\left(\frac{x_0}{2\delta} - 1\right) \tag{36}$$

In terms of the generated energy, $E_G = E_0\left(\frac{x_0}{2\delta} - 1\right)$. Therefore

$$E_K = \frac{E_G}{2} \tag{37}$$

This result merely states that the total kinetic energy of both conductor plates must equal the desired generator energy. It is interesting to calculate the plate area required on the basis of kinetic energy alone; that is,

$$w\ \ell \geq \frac{E_G}{d\rho v_G^2} \tag{38}$$

For 3-mm aluminum plates moving at 4 km/sec and a 5-MJ generator output, $w\ell \geq 364$ cm^2. It is evident that the thermal loading criterion far outweights the kinetic energy requirement.

SECTION IX

MAXIMUM CURRENT PER UNIT WIDTH

The thermal loading criterion can be recast in terms of maximum current per unit width. Such a formulation is useful in considering the output transmission lines as well as the driver plates. Equation 29 may be rewritten

$$w\,\ell \geq \frac{2E_G}{C\rho\Delta T x_0} = \frac{2E_G/\tau}{C\rho\Delta T v_G} \tag{39}$$

In the derivation of equation 29, E_G includes in addition to the energy in the load L, the resistive energy term. To first order in k, the latter term is 2k times the load energy according to equation 27. Thus, at peak current $J\ (t = \tau)$, we may write

$$E_G/\tau = 1/2\ (L_1/\tau)\ (1 + 2k)J^2 \tag{40}$$

It is convenient here to express L_1 in terms of parameters characterizing the initial generator inductance, L_0, and the ideal theoretical energy multiplication ratio, α_0, as defined just after equation 17. Then

$$L_1 = L_0/(\alpha_0 - 1) \tag{41}$$

$$L_0 = \mu_0 x_0 \ell/w = \mu_0 v_G \tau \ell/w \tag{42}$$

We obtain from the three preceding equations

$$E_G/\tau = \frac{\mu_0 v_G \ell (1 + 2k)J^2}{2w(\alpha_0 - 1)} \tag{43}$$

Substitution of equation 43 into 39 leads to the following two expressions.

$$w \geq \frac{\mu_0(1 + 2k)J^2}{(\alpha_0 - 1)C\rho\Delta T} \tag{44}$$

$$\frac{J}{w} \leq \left[\frac{(\alpha_0 - 1)C\rho\Delta T}{\mu_0(1 + 2k)}\right]^{1/2} \tag{45}$$

Equation 45 sets an upper limit on linear current density if the conductor temperature rise is to be held within a value ΔT, taken here to keep the material below its melting temperature.

For aluminum with $C\rho\Delta T \cong 1.6 \times 10^9 J/m^3$ and $\alpha_0 = 5$ MJ/300 kJ = 16.7, we have

$$J/w \leq 1.4 \text{ MA/cm}$$

For other materials such as copper or tantalum, $C\rho\Delta T$ is larger and the thermal loading limitation is more favorable. Again the analysis is based upon a fixed inductive load rather than the discharge load. However, it should be adequate for qualitative purposes.

There is another factor which enters into the limitation of current per unit width in the conductors which are not driven by explosive pressures. The magnetic pressure on the conductors reaches 40 kb at a current density of about 0.8 MA/cm and 160 kb at about 1.6 MA/cm. Depending upon the time scale of the current buildup, these pressures can move the conductors enough to increase the inductance appreciably during the last part of the generator run. As a result, the output into a low impedance load is lowered and in fact may be limited to some maximum value owing to this effect alone. Experience at Los Alamos Scientific Laboratory (LASL) with a large variety of generators and high field systems indicates that the 1.5 MA/cm limitation from thermal loading criteria is also a reasonable limitation for the fast plate generator from the viewpoint of magnetic forces.

Finally, the effects of the initial energy input should be mentioned. As pointed out in reference 4, an initial current in the generator gives rise to forces which can bow the driver plates and crack explosive materials in contact with them. The subsequent acceleration of the driver plates may deviate from planarity enough to impair the generator performance. There are several techniques for avoiding or offsetting such effects, but they must be taken into account as part of the engineering design.

SECTION X

DISC GENERATOR CONFIGURATION

The discussion so far has been directed toward the plate generator. The section on current per unit width can be applied approximately to the disc generator provided that ratio of the outer to the inner radius is not too much greater than one. Then the disc generator may be considered as a plate generator bent around in a circle with the circumference of the inner conductor replacing the width of the plate generator.

The disc generator geometry offers some possible advantages over the plate generator. The current output has a coaxial configuration which mates well with the coaxial foil load. It should be relatively easy to maintain good current and voltage symmetry with minimum waste inductance. The disc system also can be made more compact than the plate generator.

One of the most likely trouble spots in the disc generator is the interaction between the moving plates and the stationary central conductor. Since the flux is concentrated near the post, good compression in this area is vital to efficient operation. Any jetting or spray in this region could lead to a breakdown or arc-over which would trap much of the flux before it could reach the load. The same sort of loss could occur if the moving conductor near the post lagged behind the rest of the disc, thus forming a cavity near the post. For these reasons, the experimental work to be discussed in section VII was instituted. It should be noted that the higher magnetic pressure in the central region can also lead to cavity formation. However, this effect can be investigated only under the conditions of full current loading. Such work must be left to a later study.

SECTION XI

EXPLOSIVE SYSTEM

The technology exists at LASL to provide a compact explosives and initiation system which should fit the requirements of both the generators discussed in this report. The explosive is PBX 9404--a high-energy plastic-bonded explosive which can be machined to high tolerances. About 3.8 cm of 9404 in thickness is necessary to achieve the velocity and smoothness necessary. The initiating system is capable of meeting the simultaneity and uniformity requirements. The present cost for a 13.2 cm square module is about $200. It is possible that this cost can be reduced somewhat in future work. Assuming that 24 such modules might be required for a 5-MJ system, the explosives cost would be around $4800. The immediate availability of this system is one of the factors which lead to the choice of plane systems for the feasibility study. Based upon an explosive weight of 30 kg and an energy of 4.5 MJ/kg, the efficiency of conversion of chemical to electrical energy would be about 3 percent.

Calculations of velocity and distance versus time have been performed based on the explosive system just discussed. Driver plates of aluminum and copper in several thicknesses were assumed. The distance versus time plots are shown in figures 15 and 16. The free-surface velocity versus time plots are not shown since the shock structure makes them difficult to use effectively. The framing camera shots discussed later show good agreement with the calculations for 3.2-mm-thick aluminum plates.

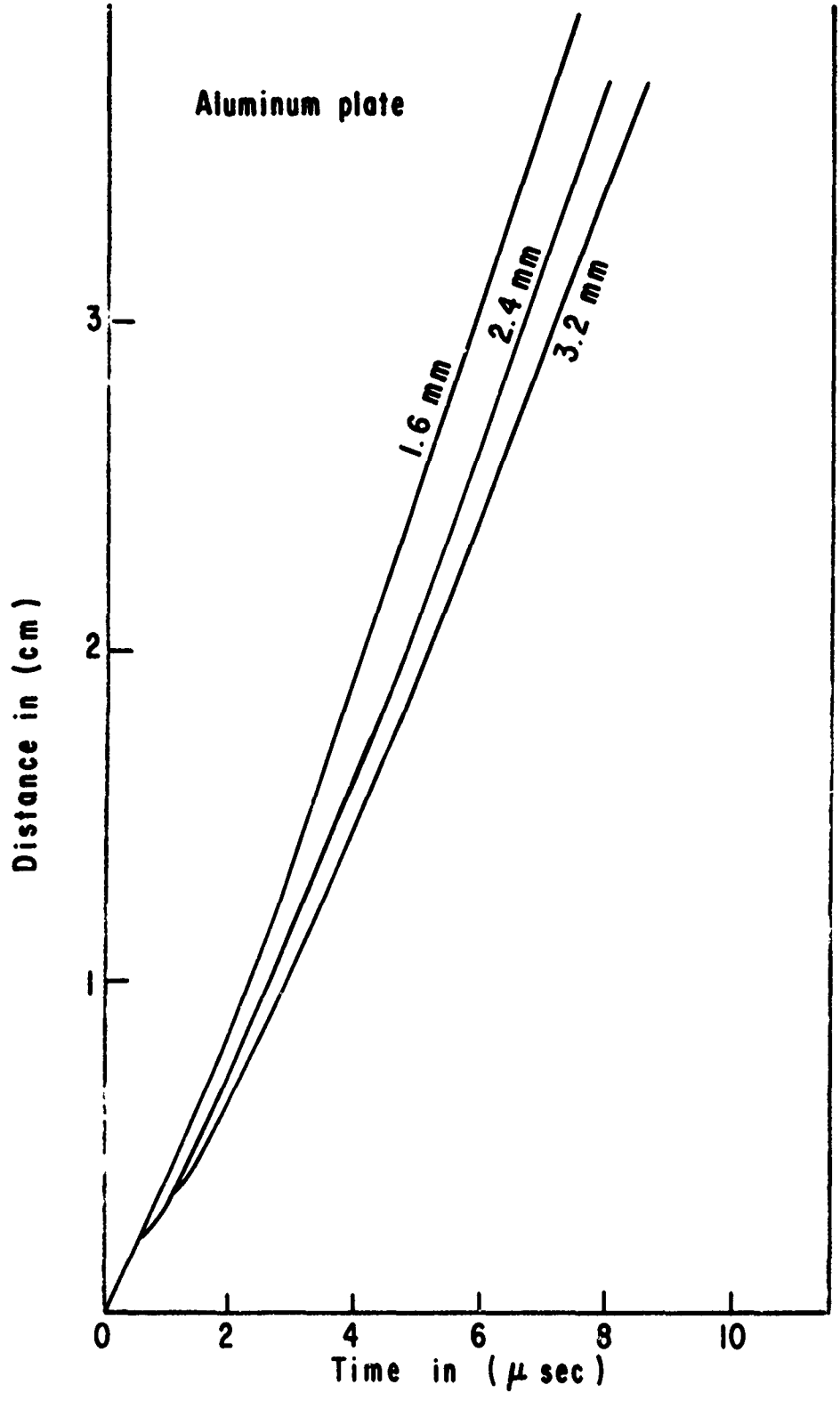

Figure 15. Distance versus time plots for aluminum driver plates. The shock hydrodynamic calculations were performed assuming 2.54 cm of 9404 explosive backed by a rigid wall. This approximation gives a good match to the actual explosive system.

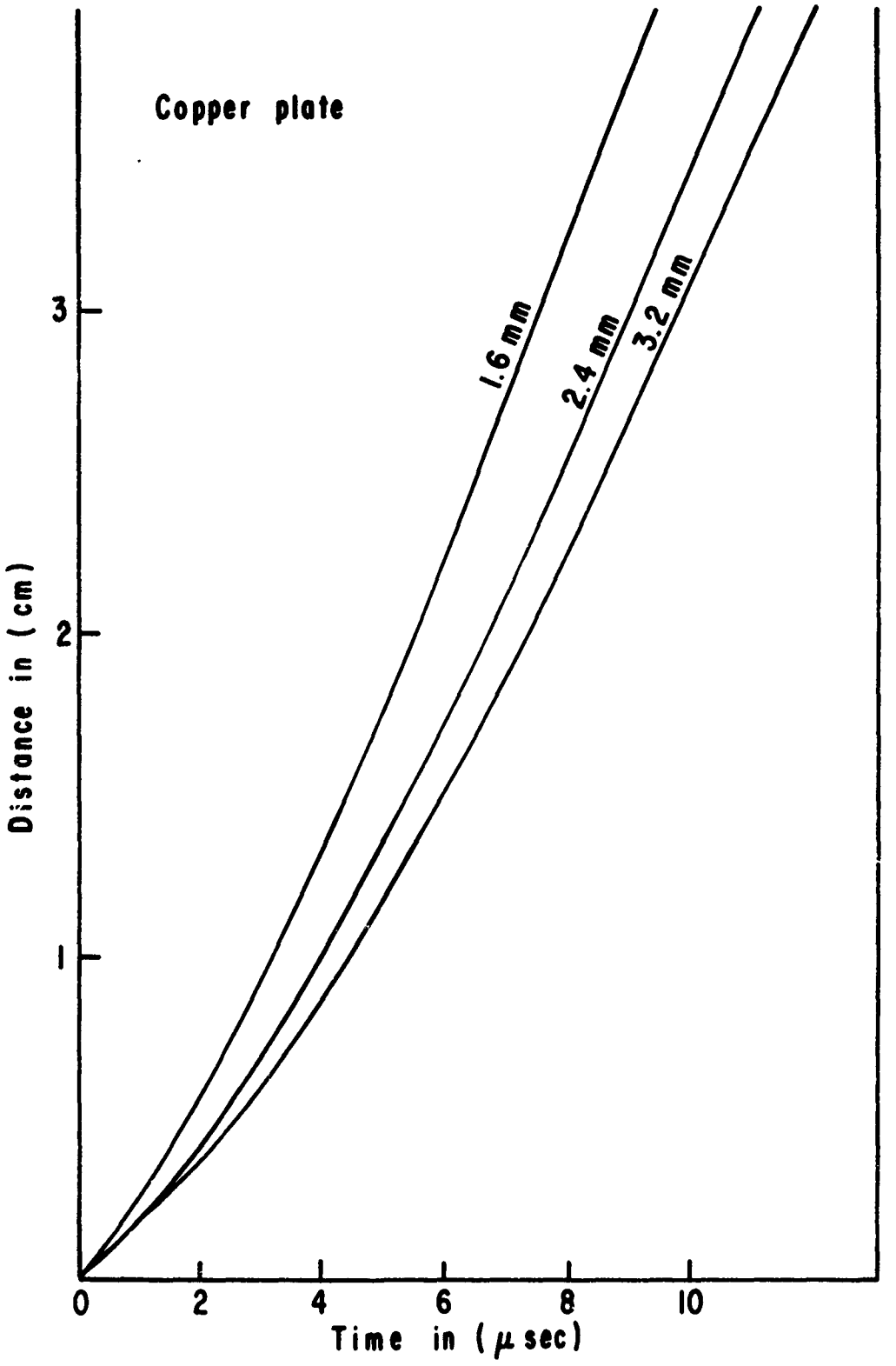

Figure 16. Distance versus time plots for copper driver plates. The assumptions were the same as those for the aluminum driver plates notes in the caption of figure 15.

SECTION XII

EXPERIMENTAL WORK

As discussed in section X, the disc generator system should have some useful features that the plate system does not. However, it was realized that the interaction between the moving conductor and the stationary central post could be a possible trouble area. For this reason, eight shots were fired to study the effect on the postplate interaction of using various materials and shapes for the post.

Figure 17 shows a schematic diagram of the shot setup for the first two shots. The 3.2-mm aluminum plates were driven by a plane wave generator and 2.54 cm of 9404. The framing camera looked through the assembly, which was backlit by an argon flash, in a direction parallel to the plate surfaces and perpendicular to the direction of motion. Figure 18 is an enlargement of one of the frames taken from the record of a shot in which the post was also made of aluminum. A fine spray or "fluff" on the surface of the plate is evident, but, in addition a spray of material can be seen which is running well ahead of the plates. It is evident that the collision of the jet material at the midplane would result in a conducting path in parallel with the post and the subsequent trapping of flux. This situation could lead to serious losses, since the flux density is highest near the post. Figure 19 is similar to figure 18, except that a tantalum post was used in the shot. Some jetting is evident, but much less than in the case where an aluminum post was used.

Figure 20 shows the shot setup used for most of the remaining experiments. Only one driver plate and explosive assembly was used so that the framing camera could look in at an angle and minimize the obscuring effects of the surface spray. Mirrors were employed to obtain stereo pairs on each frame.

The third and fourth shots were fired using the framing camera alone and were designed to observe the effects of a slight taper on a tantalum post. There were no observable differences between the shot using a straight post and the shots using tapered posts. The records are not reproduced here since they are similar to those from which figure 23 is taken.

The remaining four shots made use of 450-kV flash x-ray equipment in conjunction with the framing camera as shown in figure 20. Figure 21 is a stereo pair of the shot using an aluminum post and figure 22 is the corresponding x-ray picture. Figures 23 and 24 show the same sequence for the tantalum post. It is evident that, in addition to the spray of material (probably aluminum) thrown out at the corner between the post and plate, a cavity is formed around the post. This cavity implies a poor contact with the plate--a serious matter since this region would carry high current densities in an actual generator. However, the tantalum post induces less cavitation and again seems to be a better candidate than the aluminum.

The last two shots were designed to show the effects of some simple geometry changes on the interaction with the tantalum rod. In the next experiment, the tantalum post was inserted in a hole in the plate so that it was flush with the back surface. The results are illustrated in figures 25 and 26. It is evident that the cavity is smaller yet than it was in the previous shot. The last shot used a post with a hemisphere machined on the end which was set into a hemispherical cavity extending halfway through the aluminum plate. Since the depth of the hole in the plate was less than the radius of the hemisphere, a portion of the post formed an overhang above the plate. The framing camera pictures in figure 27 indicate that an extensive spray of material comes off probably owing to the collision between the plate and the portion of the hemisphere which overhung the plate. The x-ray picture of figure 28, however, indicates that the cavity has closed up considerably.

There was no opportunity to try further design variations within the rather limited scope of this study. However, it does seem that there is a possibility of eliminating the spray and the cavity by an experimental shot program supported by two-dimensional hydrodynamics calculations. Certainly, some improvements were effected by the rather simple techniques employed in the present series. It should be mentioned, however, that the behavior observed here could be quite different when the driver plates and posts are carrying large currents.

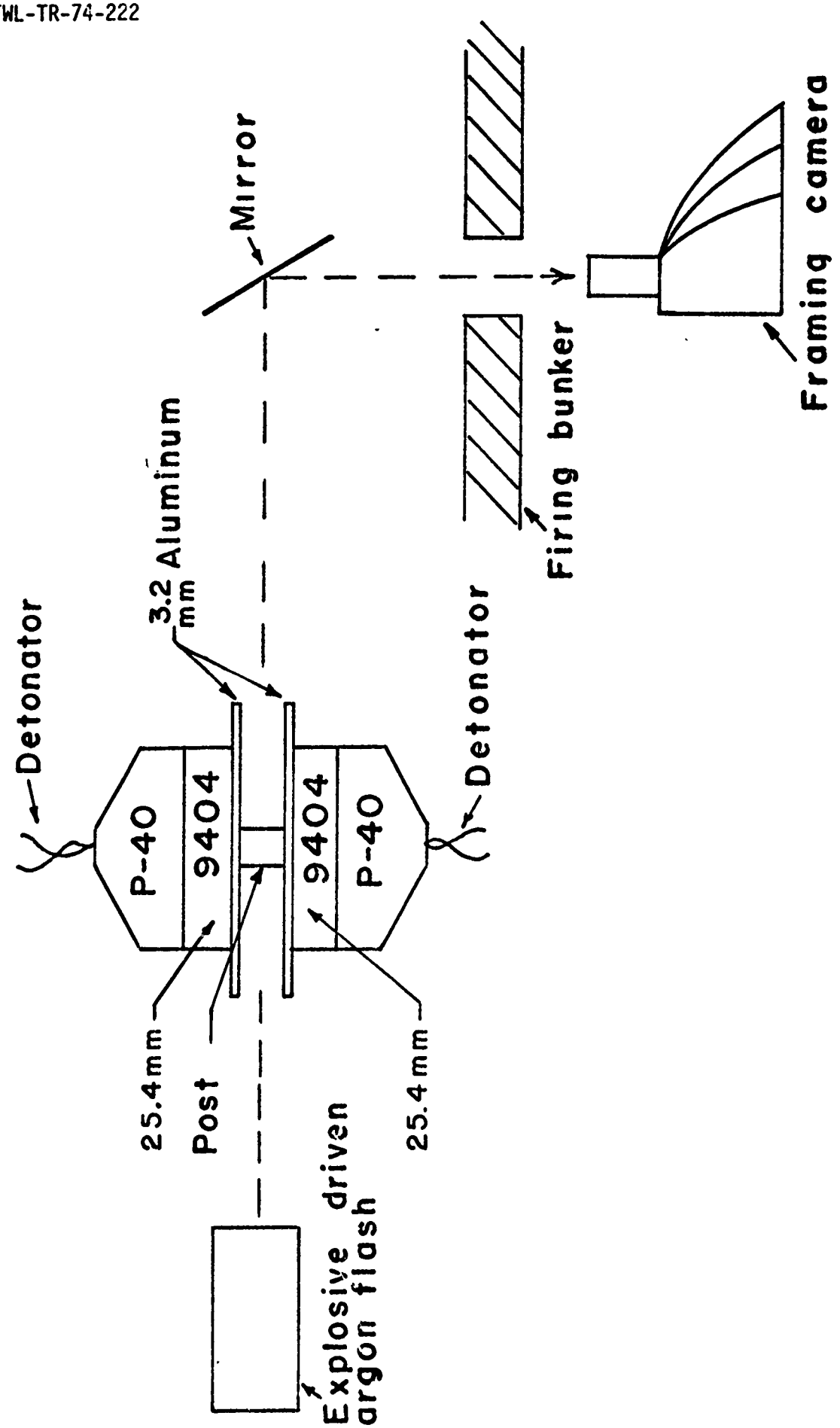

Figure 17. Schematic diagram of the shadowgraph technique used in the first two shots.

SECTION XIII

SUMMARY AND CONCLUSION

It appears feasible to use high energy, short pulse explosive generators to drive electromagnetic implosions. It was shown that transfer of generated energy to imploding foil plasma discharges can be accomplished with efficiencies exceeding 50 percent. The numerical calculations displayed indicate that the close electrodynamic coupling of the generator and load providing such efficiencies requires proper timing of the energy delivery to the load and the load dynamics. In particular, the generator should deliver its energy to the load in a time about equal to the discharge implosion time ($\leq$ 1 μsec) for high plasma temperatures to be obtained. To accomplish this merely requires closing a switch to the load after about 70 percent of the run of a moderately fast generator has been completed. The nature of the foil-plasma is such that high generator currents are obtained and large amounts of energy can be transferred from the explosive to the plasma. Implosion speeds in excess of 100 cm/μsec and kinetic energies exceeding 10 MJ are computed. Plasmas with such speeds and energies can be used to compress other plasmas, and/or magnetic fields, or as hign power, prompt radiation sources ($P_{rad} > 10^{14}$ watts).

Detailed consideration was given to varicus factors limiting generator performance. It is seen that high voltages are developed during generator operation associated with the transfer of energy to the dynamic load. Voltages in excess of 200 kV, however, are only present for very short times ($\sim$ 50 nsec), so that inclusion of insulating material (SFs and Mylar for example) in the interconductor gap should be sufficient to inhibit internal arcing.

For short pulse ($\leq$ 5 μsec), high energy generator operation, thermal loading of the conductors rather than magnetic retardation of their motion appears to be the dominant process which determines the generator plate area, and thus the explosive area. For rectangular plate generators, an efficiency of utilization of high explosive of a few percent is estimated.

A new generator configuration involving the use of a flat disc driven over a stationary center post was considered and possible advantages were discussed. Feasibility of the disc generator configuration depends considerably upon the

character of the interaction of the explosively driven thin conductor plates with the stationary post. Experimental study indicates that some jetting and cavitation occurs in the interaction region, with less of this effect observed when tantalum is used instead of aluminum for the post, particularly if the tantalum post has a hemispherical end and is inserted into the aluminum plate.

Further experiments are required to determine: (1) the maximum current per unit width, J/w, that can be handled initially in a rectangular plate system; (2) the maximum J/w such a system can provide under fast explosive compression; and (3) the interaction of plate and post under various situations of tapering, insertion, etc., and with strong current conduction to evaluate fully the disc generator configuration. In addition to this work, experiments are needed to verify the behavior of EM implosions at high energies and currents.

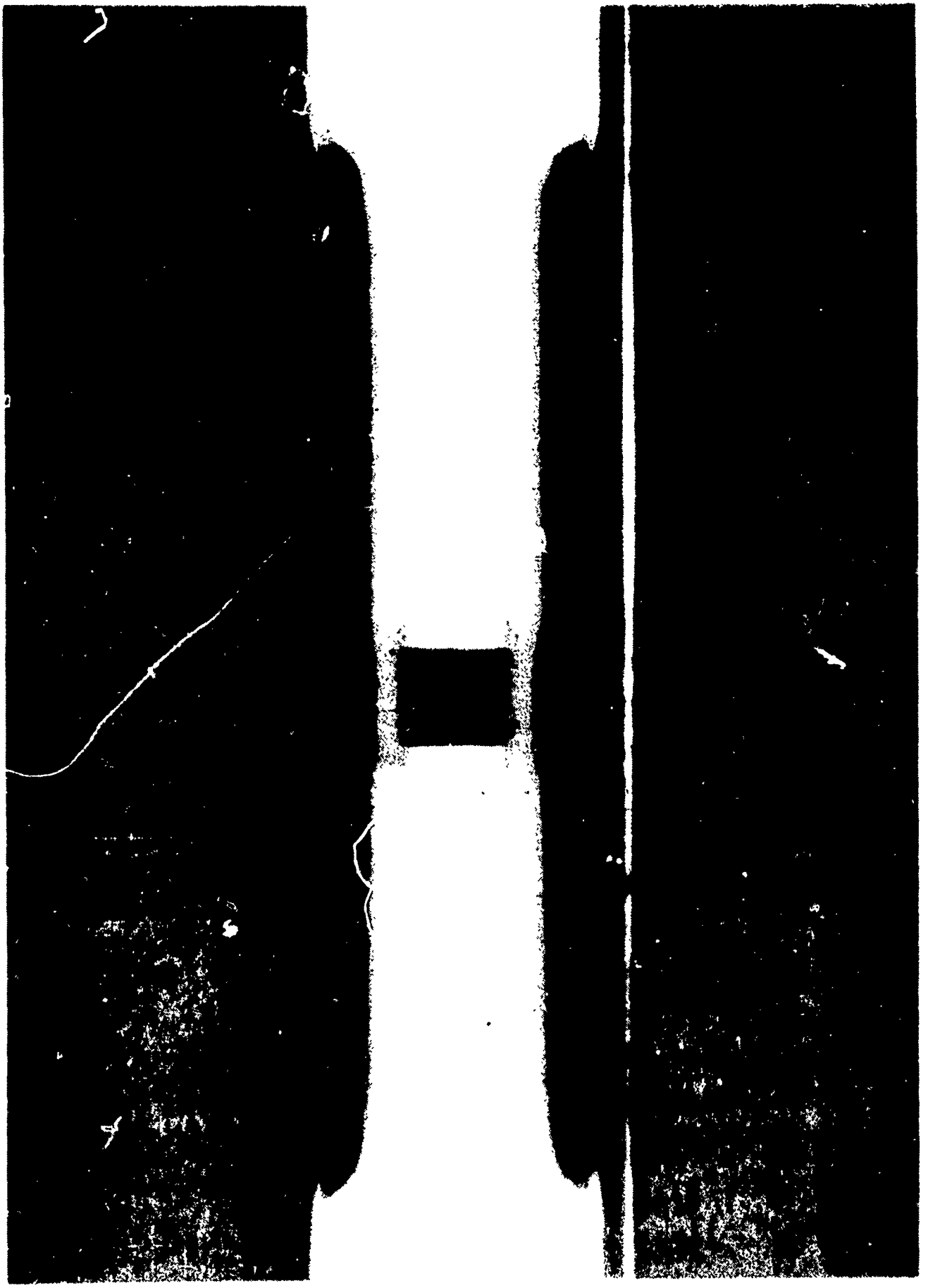

Figure 18. Shadowgraph framing camera picture showing the interaction of aluminum driver plates with an aluminum post. The fuzzy appearance of the plate surfaces is the result of a fine spray of material which is often seen in such shots.

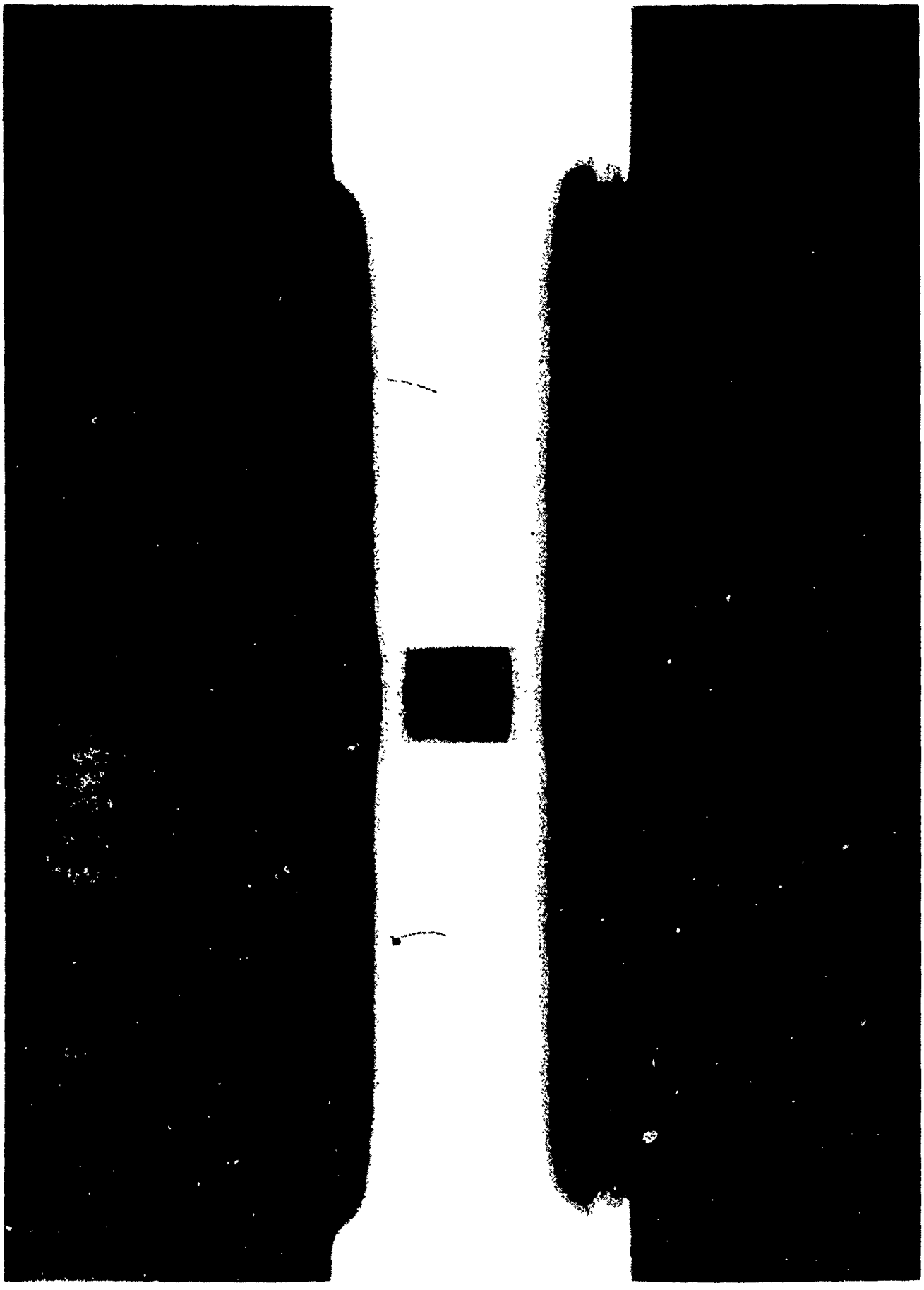

Figure 19. Shadowgraph framing camera picture showing the interaction of aluminum driver plates with a tantalum post. The amount of spray at the the interaction region is much less than that visible in figure 18.

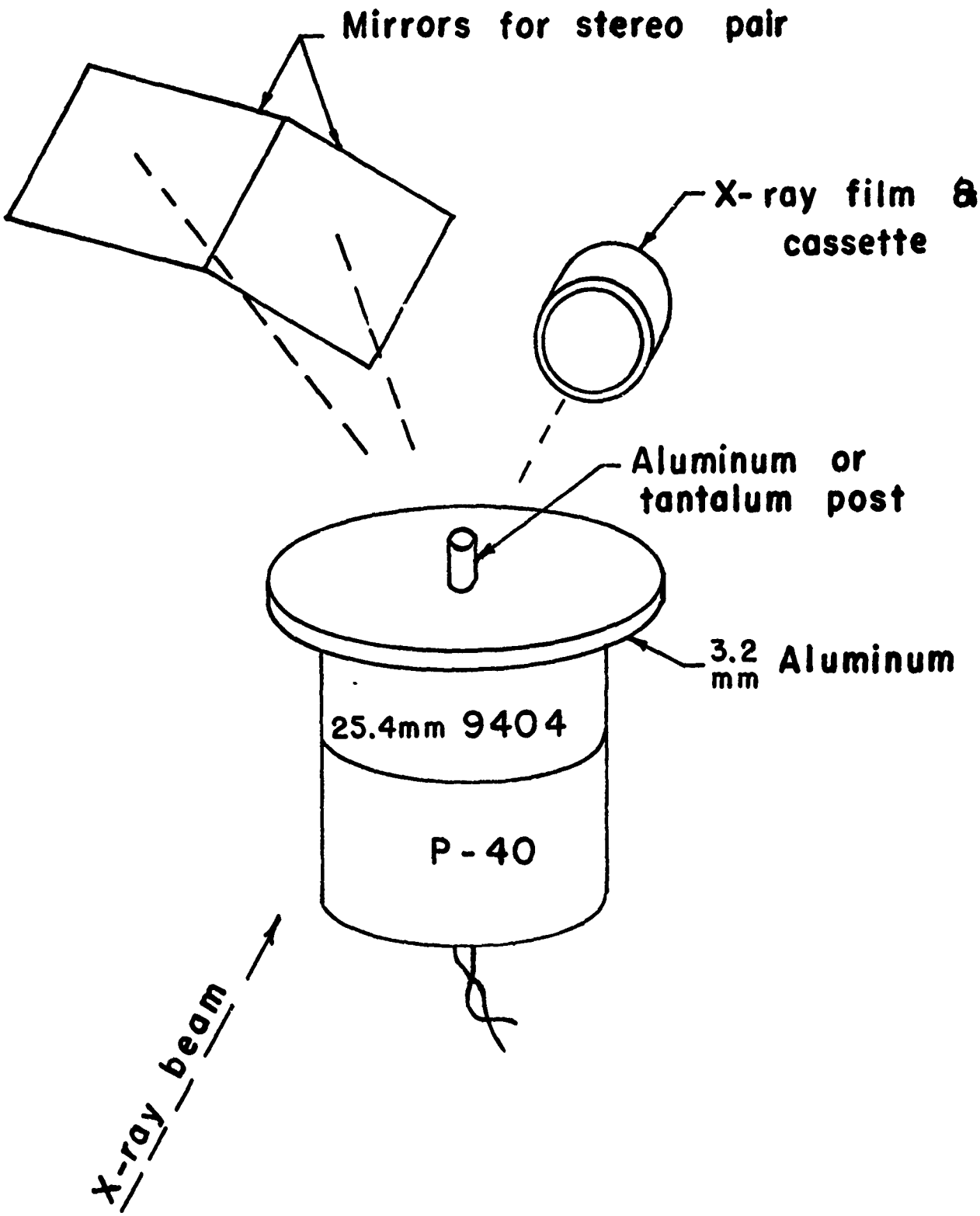

Figure 20. Schematic representation of the shot setup for simultaneous stereo framing camera pictures and flash x-ray shadowgraphs. Not shown is the explosive-driven argon flash which illuminates the shot assembly.

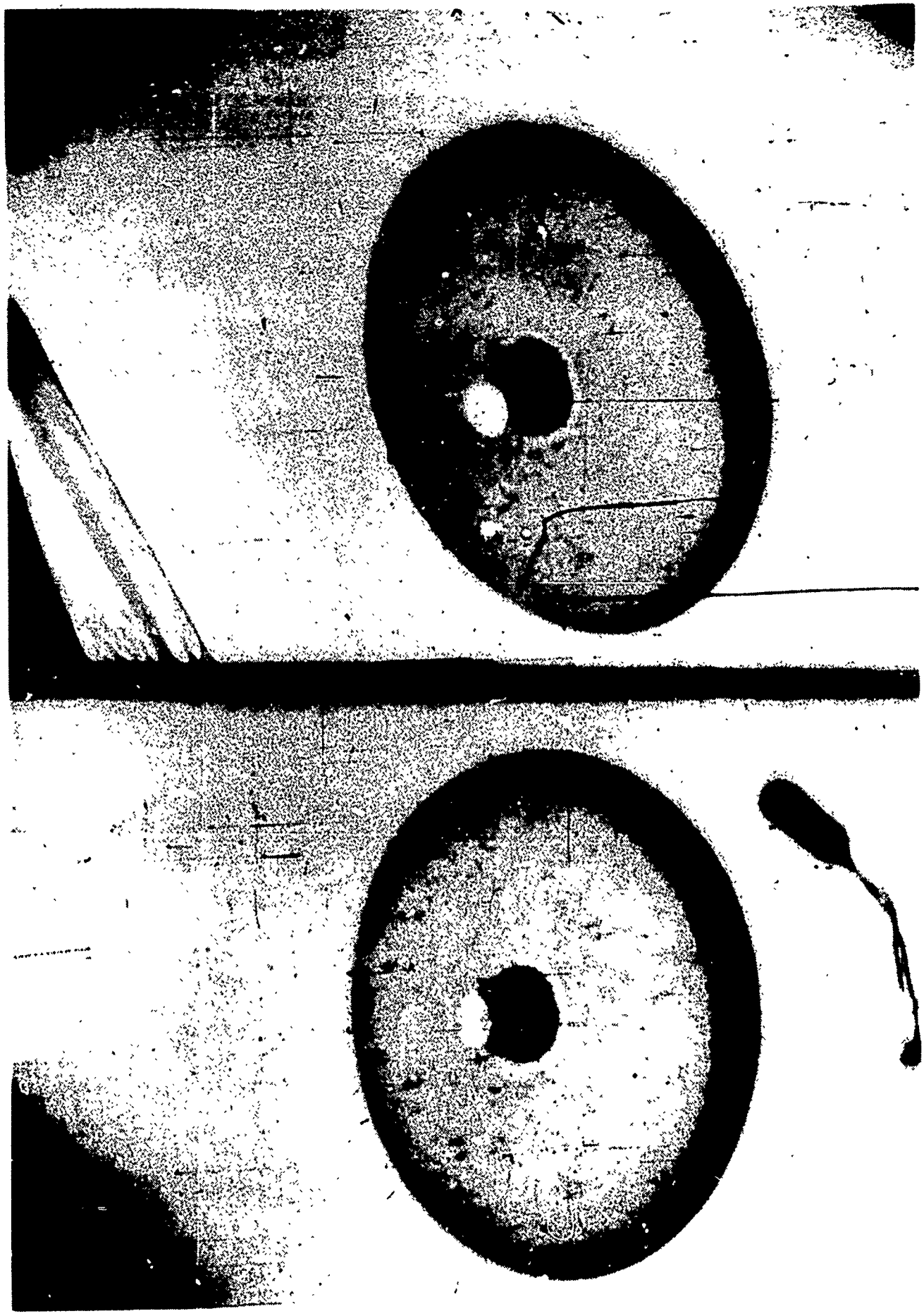

Figure 21. Stereo framing camera pictures of the interaction between an aluminum driver plate and an aluminum post. The spray from the interaction region is quite evident.

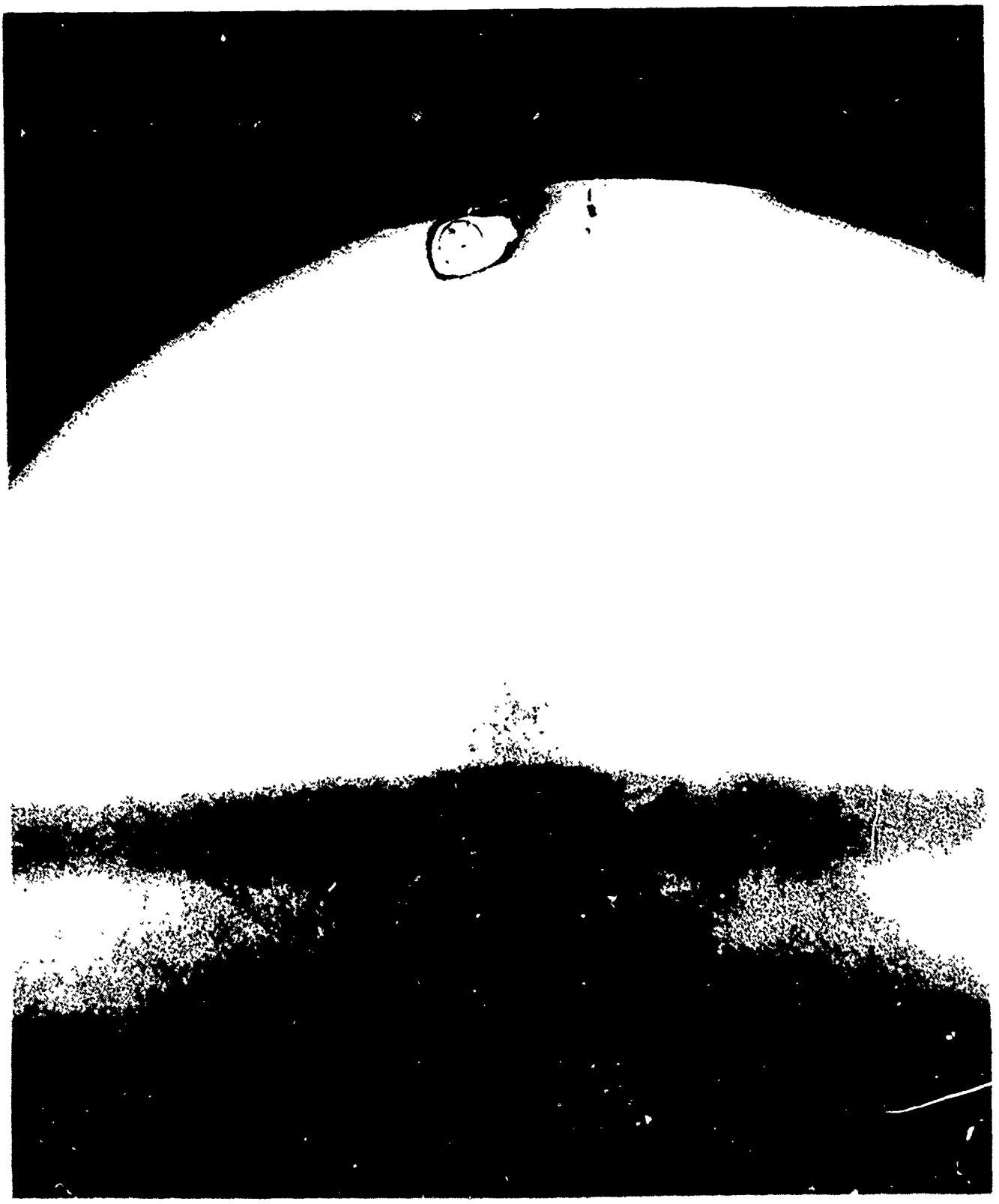

Figure 22. Flash x-ray picture taken at about the same time as the framing camera picture in figure 21. The image is faint because of the low stopping power of the aluminum, but it is possible to make out faint traces of the spray and a cavity around the post.

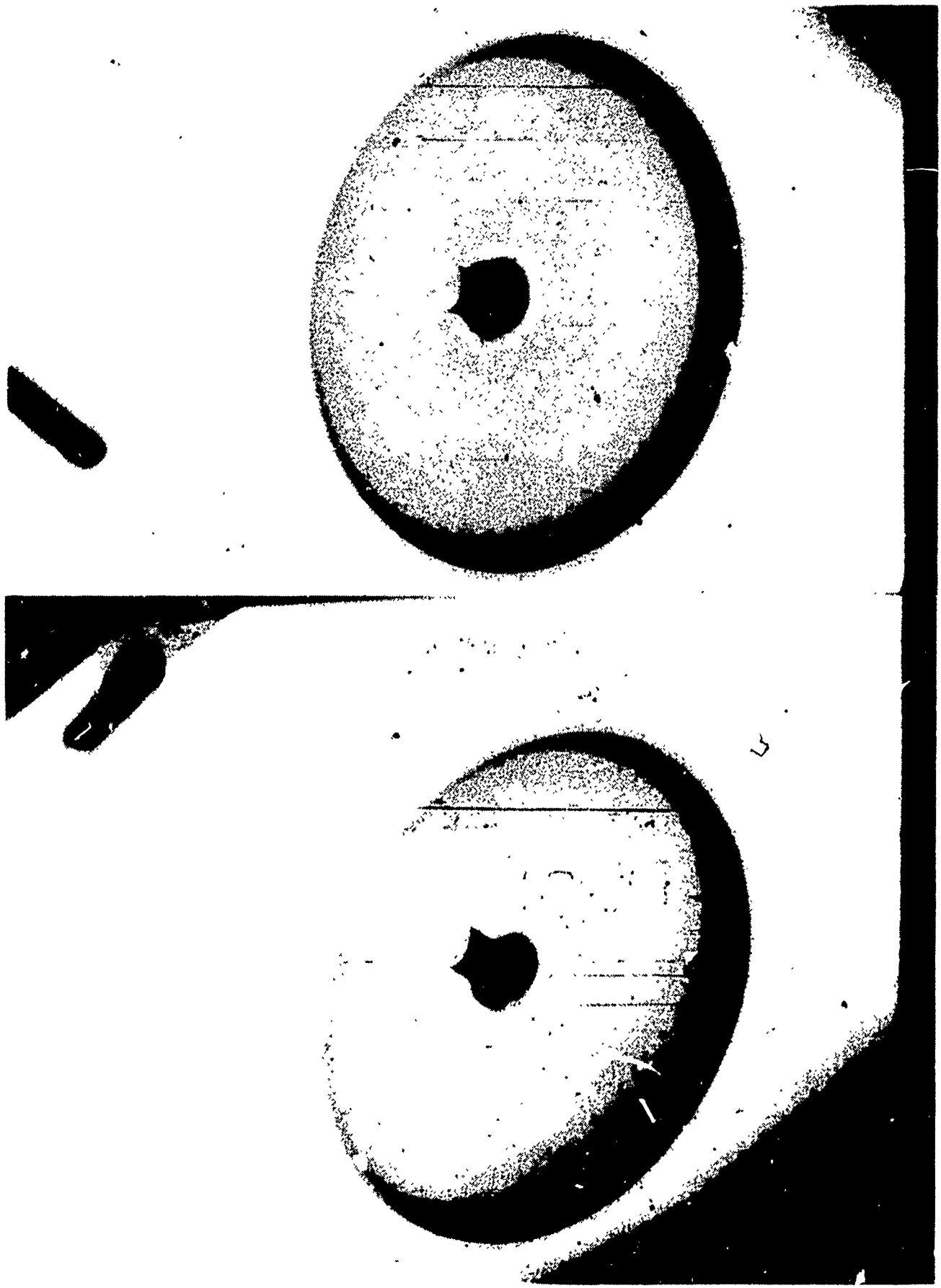

Figure 23. Stereo framing camera pictures of the interaction between an aluminum driver plate and a tantalum post. The spray from the interaction zone is less than in the shot using the aluminum post.

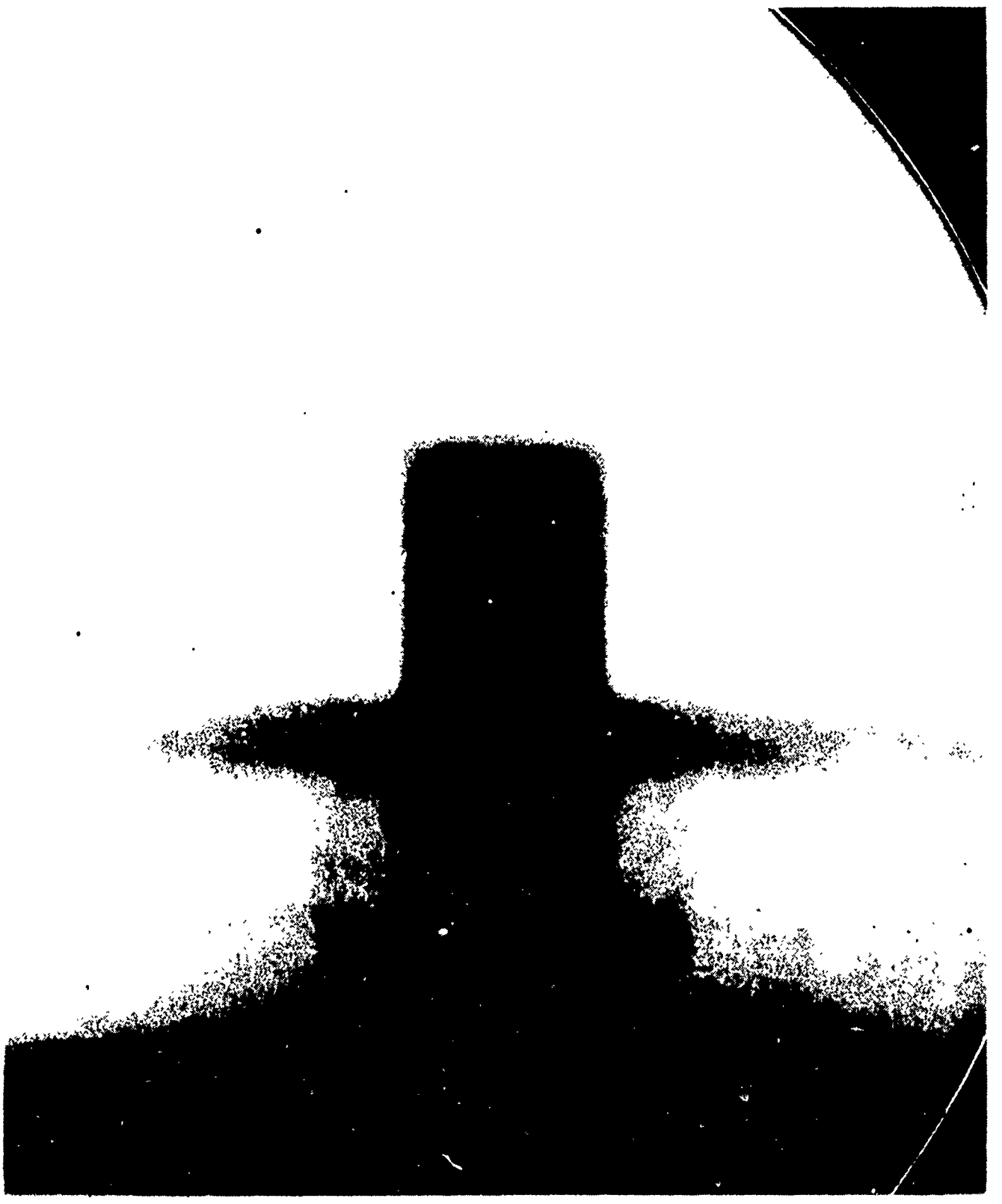

Figure 24. Flash x-ray picture taken at about the same time as the framing camera pair shown in figure 23. The spray is less evident and the cavity smaller than was the case for the aluminum post.

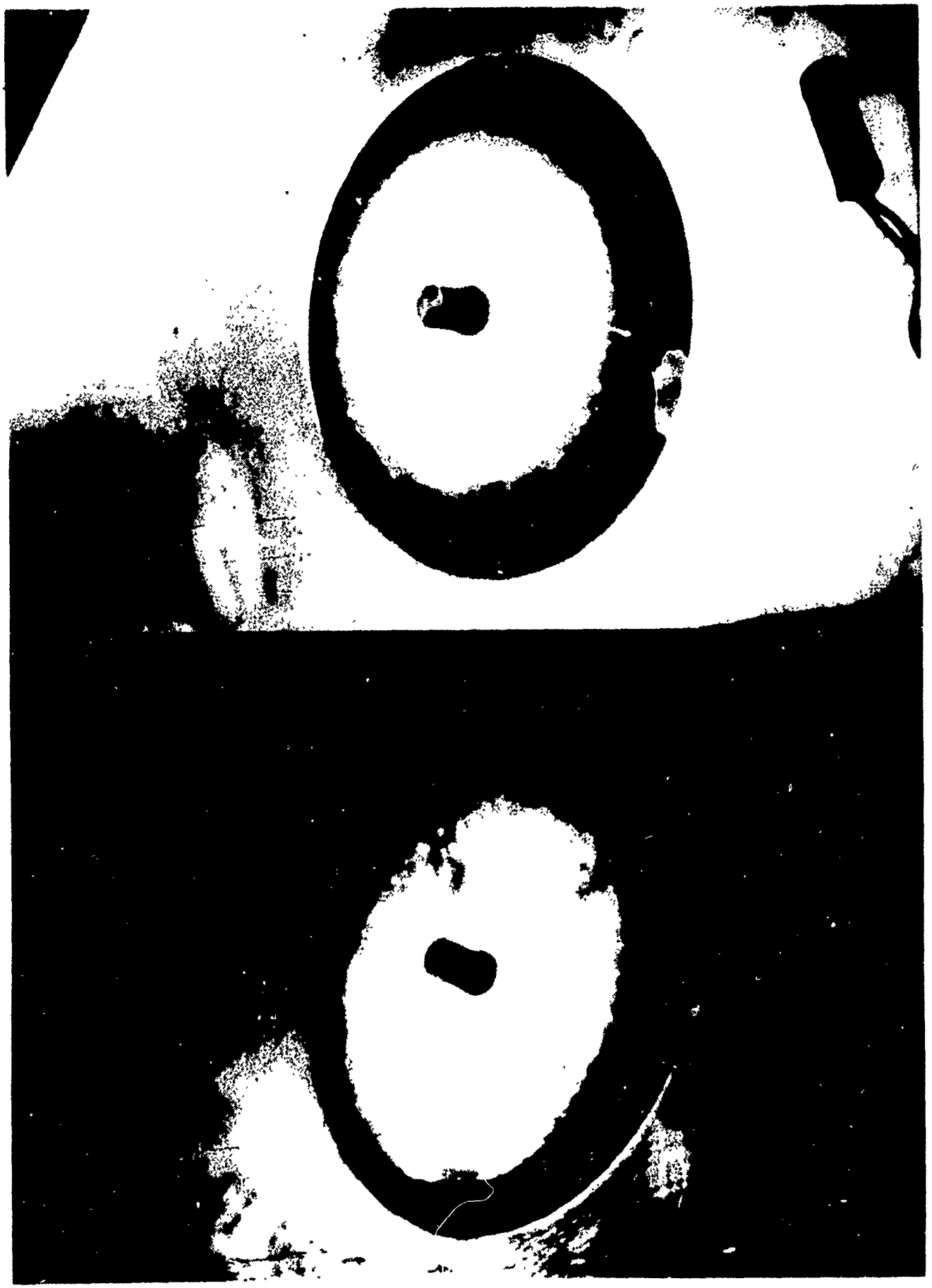

Figure 25. Stereo framing camera pictures of the interaction between an aluminum driver plate and a tantalum post which was recessed into the aluminum driver plate until flush with the back surface. There is less spray than in the previous shots.

Figure 26. Flash x-ray picture corresponding to the framing camera pictures of figure 25. The cavity area has decreased by comparison with the previous shots.

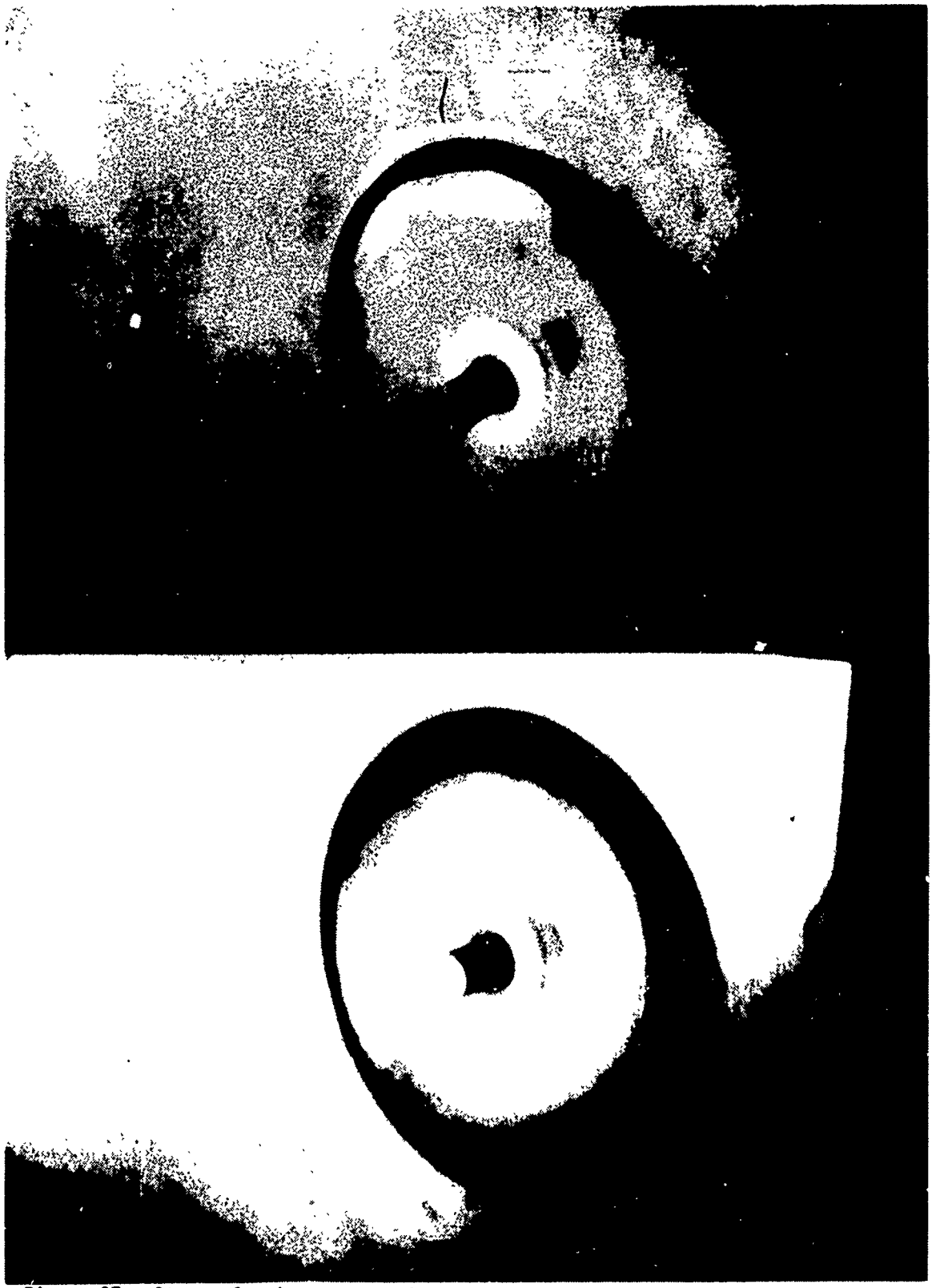

Figure 27. Stereo framing camera pictures of the interaction between an aluminum driver plate and a tantalum post with a hemispherical end recessed halfway into the driver plate. Much of the ring of material visible in the photographs probably arises from the collision between the driver plate and that portion of the hemispherical cap which overhangs the front surface of the plate.

Figure 28. Flash x-ray picture corresponding to the framing camera pair of figure 27. The cavity appears to have closed almost entirely.

REFERENCES

1. P. Turchi and W. Baker, Generation of High Energy Plasmas by Electromagnetic Implosion, AFWL-TR-73-56, Air Force Weapons Laboratory, Kirtland Air Force Base, Albuquerque, New Mexico.

2. J. W. Shearer, et. al., J. Appl. Phys., 39, 2102, 1968.

3. C. M. Fowler, R. S. Caird, W. B. Garn, and D. E. Thomson, High Magnetic Fields (edited by H. Kolm, B. Lax, F. Bitter, and R. Mills), Technology Press, Cambridge, Massachusetts, p. 275, 1962.

4. F. Herlach, H. Knoepfel, and R. Luppi, Conference on Megagauss Magnetic Field Generation by Explosives and Related Experiments, Frascati, Italy, European Atomic Energy Community, Brussels, p. 287, 1966.

5. H. Knoepfel, Pulsed High Magnetic Fields, North-Holland Publishing Company, Amsterdam, p. 183, 1970